FLEXURAL WAVE PROPAGATION THROUGH JOINTS IN (PMMA) BEAMS AN EXPERIMENTAL APPROACH

A Thesis Submitted

In Partial Fulfilment of the Requirement

for the degree of

MASTER OF TECHNOLOGY

by

MAHENDRA PRATAP SINGH

to the

DEPARTMENT OF AEROSPACE ENGINEERING

INDIAN INSTITUTE OF TECHNOLOGY

KANPUR

JUNE 1994

31 AUG 1994 / AE

KANPUR

Acc. No. A. 118172

AE - 1994 - M. SIN - FLE

A118172

CONTENTS

ACKNOWLEDGEMENT

I wish to express my profound gratitude to Dr. SUDHIR KAMLE for whose invaluable guidance, constant encouragement and advice at every stage of my thesis made this work possible.

I am extremely indebted to Dr. ANIL KUMAR of Chemical Engineering allowing me to use various facilities at POLYMER Laboratory for experiments and for providing invaluable guidance in my experiments.

My special regards to my classmates SIMANT, CHAVELI, SHAFI and VERMA and to all who have given help and encouragement in thesis preparation. I can offer here a most humble acknowledgement of appreciation.

Finally I must express my deepest sense of gratitude to my parents for their constant help and encouragement.

Support of ARDB in funding of this thesis is gratefully acknowledged.

MAHENDRA PRATAP SINGH

INDIAN INSTITUTE OF TECHNOLOGY

KANPUR

June 30, 1994.

CERTIFICATE

This is to certify that the present work on "FLEXURAL WAVE PROPAGATION THROUGH JOINTS IN (PMMA) BEAMS, AN EXPERIMENTAL APPROACH" has been carried out under my supervision and that it has not been submitted elsewhere for a degree.

DR. SUDHIR KAMLE
Associate Professor
Department of Aerospace Engineering
Indian Institute of Technology
Kanpur - 208016, INDIA.

June 30, 1994.

LIST OF FIGURES

LIST OF TABLES

ABSTRACT

Cuts were made in a 840 mm x 25.4 mm x 5 mm Polymethylemethacrylate (P.M.M.A.) beam which were joined using Ethylenedichloride. The joint thus formed is ultrathin and can be approximated to be of zero thickness. Viscoelastic property of interfacial region has been varied by adding plasticizer Dioctyle Phthalate to Ethylenedichloride. For controlled force applied, transverse wave's acceleration (measured at different locations on the beam) consists of the forward propagating wave, reflected wave from joint, reflected wave from end and doubly transmitted through the joint; and the reflected wave from other end. At any given location these waves are seperated in time and Fast Fourier transform of these waves was taken for locations before and after the joint. Results show that the amplitude gain in dominant frequency decreases as the plasticizer content in the joint is increased.By mechanical testing of specimens made of similar joints it has been found that ultimate strength of the joint also decreases with plasticizer content.

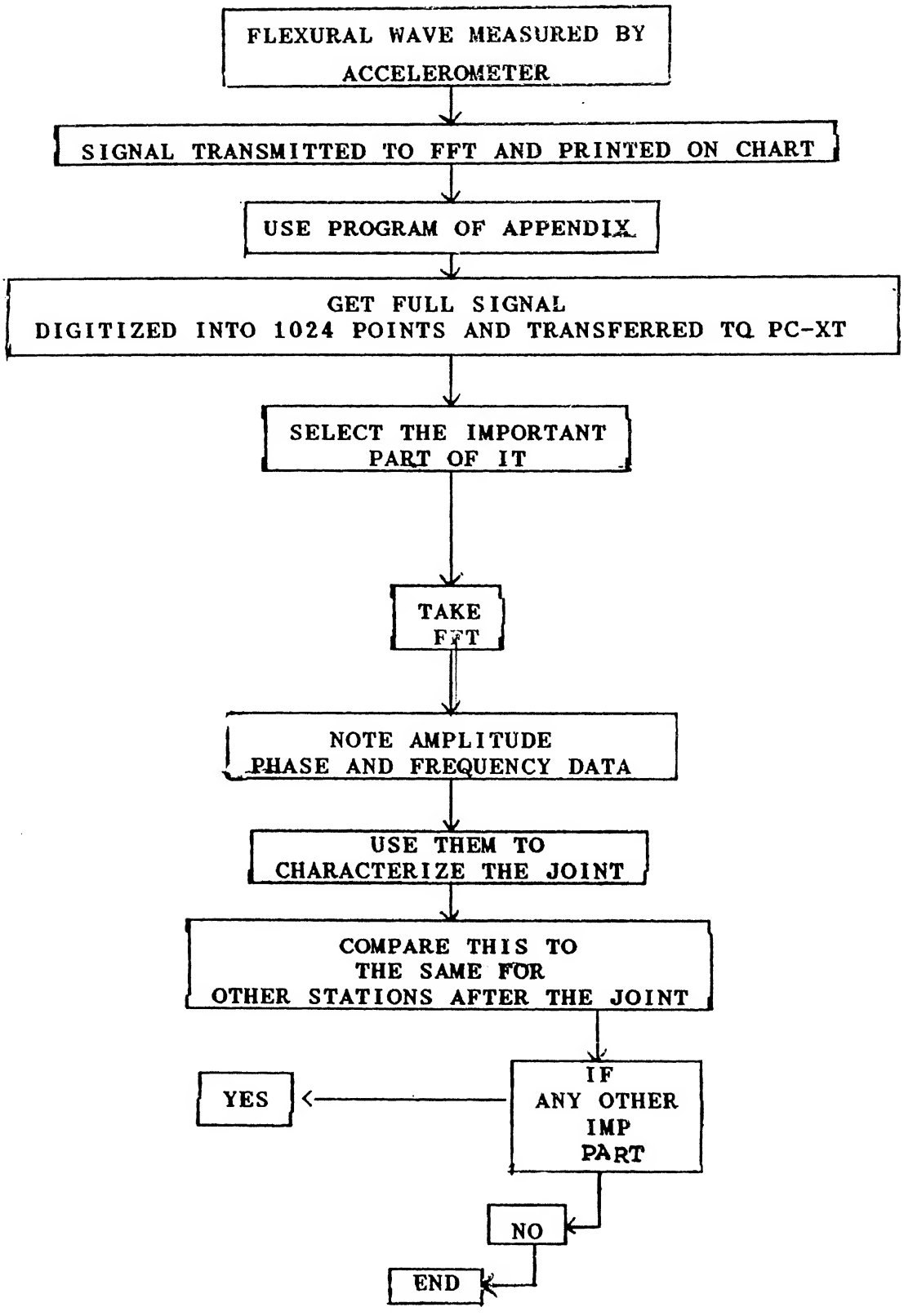

SCHEME OF PROCESSING THE FLEXURAL WAVE DATA

CHAPTER 1

Introduction

The use of adhesive bonds in primary structures is restricted due to limited growth of methodologies for predicting their life. It is desired to develop nondestructive testing technique (NDT) to establish quantitative relations between the materials structure and its mechanical performance[1-5]. Among various NDTs. the commonly used techniques are pulse echo through transmission, C scan, resonance, spectroscopy, vibrations under impact etc. All nondestructive testing procedures proceed in two stages : in the first one (sometimes called the forward problem) we determine wave speed for given joint properties. In the reverse problem, we make measurements of wave speed through joints and use this information to find out the joint properties (i.e., the adherend thickness and wave speed in it, the adhesive thickness and the wave speed in it and the modulus).

The important characteristics of joints is that there is a definite limit to the bond strength developed between specified adherends for a particular adhesive[6-10]. If it is decided to use double overlap joints, the load capacity increases with increase in overlap until a limiting value is attained. Beyond this overlap, no more load transfer can be achieved. Experiments have shown that load transfer is mostly confined to the two end zones with a lightly-loaded elastic troughs in between. The second inherent characteristics of the joint is that the maximum potential bond shear strength is determined by the adhesive strain energy in shear per unit bond area. This is shown to be very important criteria. The precise shape of the stress-strain curve has been

shown to have little effect on the limiting joint strength. Joint efficiency charts are provided for common adherend materials. Since the adhesive films behave differently under peal and shear, the results shown in them can at times be misleading. For moderate thicknesses, the limiting shear strength of the adhesive may limit the joint strength. As opposed to this, for thicker adherends, the limiting strength is invariably the peal strength.

When a joint undergoes a fracture, the failure could occur either because the adhesive has failed or the interfaces between the adhesive and the adhearend has failed[11-21]. The former is called cohesion failure to distinguish from the latter called adhesion failure. In an actual joint the failure normally occurs by a combination of both these. The failed joints have been examined under the microscope and invariably the failure is initiated at the microvoids created either by the air entrapped or the reaction products released during the curing of the adhesive.[14-16]

Commonly encountered bonding problems can be classified into following types : debonding, cohesive weakness and interface weakness. Debonding includes voids and complete sepration of the adhesive and adherends. This situation can normally be detected by the techniques of pulse echo, through transmission, C-scans etc., cohesive weakness by techniques as resonance, spectroscopy etc. As opposed to these, the detection of interface weakness is more difficult. The adhesive and adherends could appear in physically perfect bonding state, but could lack the strength. Traditional ultrasonic techniques do not distinguish between good and bad bonds. Work has been initiated in the development of new techniques and theoretical models to understand the wave propagation at the bond interface.[28-30] Various theoretical models can

be classified into two types[25-29] : (a) a complete bond thickness weakness model and (b) interface weakness model.

The bond thickness weakness model refers to wave propagation (e.g., plate waves, leaky waves, interface waves etc.) through the adhesive layer and two larger adherends. The received signals are affected both by interface as well as by cohesive weakness. For the second type models, the interface weakness is evaluated more directly by examination of the transmission factors from the interface between the adhesive and the adherends. The existence of an interface wave has been demonstrated which has smooth contact with the adherends and the adhesive and acts as a viscous liquid layer. In another quasi-static model of a weak bond, a spring with an elastic constant and mass was assumed to connect two solid semi infinite spaces. In these models, different bonding qualities refer to different bonding conditions, such as (1) debonding, (2) kissing bonding (3) smooth (or slip) bonding (4) general weakness bonding and (5) rigid (welded or perfect) bonding.

The rigid bonding is considered as a perfect contact between two media and it assumes the continuity of traction force and particle velocity at the interface. The kissing bond assumes that the traction force and particle velocity are continuous only in the direction normal to the interface and that the tangential components of the traction force is zero. The reflection and refraction factors from a kissing bonds come out to be of frequency dependent mathematically which unfortunately is contrary to the experimental finding. The smooth bonding is of primary concern because it can easily be missed with a traditional normal beam longitudinal wave inspection procedure. The smooth bond can be easily simulated experimentally with a thin film between two

solid media. A perfect bonding in an adhesive joint can never exist and some of the major parameters that affect the bond strength are bondline thickness, surface roughness, chemical conditions, adhesive type, environmental conditions and the aging effects. The boundary layers have different physical and chemical properties.

The fracture mechanics approach has been widely used to correlate the quasi-static and fatigue crack growth behaviour of the adhesive joints. The fracture parameters are often calculated using finite element methods because the governing equations for arbitrary joint configuration loading modes in complex structure cannot be solved analytically[30-48]. One way is to treat all planar adhesive joints as comprising of one or more sandwitch elements and the free body diagram of each written. The reactions in each adherends are determined and stresses in each adhesive layers obtained using plate bending analysis.

In this work, we propose to use flexural waves generated through impacting for characterizing the joint interface. In doing this we have made the following two kinds of measurements of the flexural waves.

(a) The measurement of acceleration at a given point. In this process we have argued that the forward and reflected transverse waves are seperated in time.

(b) Comparision of forward waves at immediate points across the joint. We have taken a poly methyl methacrylate (PMMA) beams of uniform cross section and produced a cut on it. The two pieces were joined using Ethylene dichloride solvent. The viscoelastic nature of the joint was varied using a suitable plasticizer. Through our experimental analysis we have developed a correlation

between the joint property and transverse waves generated in it. Further, we have also solved problem of a viscoelastic beam clamped in middle and vibrated by a sinusoidal force[50], solution has been used for material characterization.

CHAPTER 2

SOLUTION OF FLEXURAL WAVE PROPAGATION IN VISCOELASTIC BEAMS A FOURIER TRANSFORM APPROACH.

Let us consider a uniform viscoelastic beam with a simusoidal force applied at its center. Because of the symmetry, we solve the problem of beam with force applied at one end as shown in figure 4. The governing differential equation for transverse displacement y is (For any general loading)

$$\frac{\partial V}{\partial x} = \frac{\partial^2 M}{\partial x^2} = F(x) - m \frac{\partial^2 y}{\partial t^2} \qquad (1)$$

For the viscoelastic material, the stress and strains are related in general by (in time)

$$\left[Q_o + Q_1 \frac{d}{dt} + Q_2 \left(\frac{d^2}{dt^2} \right) + \cdots Q_m \frac{d^m}{dt^m} \right] \sigma(t)$$

$$= \left[P_0 + P_1 \frac{d}{dt} + \cdots P_n \frac{d^n}{dt^n} \right] \varepsilon(t) \qquad (2)$$

where $\sigma(t)$ and $\varepsilon(t)$ are the stress strains at any given time and Q_o to Q_m and P_o to P_n known material constants. We define σ and ε in Fourier transform domains as $\bar{\sigma}(\omega)$ and $\bar{\varepsilon}(\omega)$ as follows

$$\bar{\sigma}(\omega) = \int_{-\infty}^{\infty} \sigma(t)\, e^{-i\omega t}\, dt \qquad (3)$$

$$\bar{\varepsilon}(\omega) = \int^{\infty} \varepsilon(t)\, e^{-i\omega t}\, dt \qquad (4)$$

we obtain from equn(2)

$$\bar{\sigma}(\omega) = E^*(\omega).\bar{\varepsilon}(t) \qquad (a)$$

where

$$E^*(\omega) = \frac{P(i\omega)}{Q(i\omega)} \qquad (b)$$

$$P(i\omega) = P_0 + P_1(i\omega) + P_2(i\omega)^2 + \ldots P_n(i\omega)^n \qquad (c)$$

$$Q(i\omega) = Q_0 + Q_1(i\omega) + Q_2(i\omega)^2 + \ldots Q_n(i\omega)^n \qquad (5)$$

One can show that in this domain, eqn(1) reduces to

$$E^*I \frac{d^4\bar{y}}{dx^4} + m(i\omega)^2\bar{y} = \bar{F}(\omega) \qquad (6)$$

where $\bar{F}(\omega)$ represents the Fourier transform of the force applied.

Now we consider the problem of a beam held in a clamp of mass M. The clamp is supported in such a manner that it is able to move freely in the y direction but can not rotate in the x-y plane. It is assumed that a sinusoidal force $F_o e^{i\omega t}$ is acting upon the clamp, as shown in figure 1. The boundary conditions for this systems are(a) zero bending moment at x = l (b) zero shearing force at x = l (c) zero slope of displacement at x = 0. The last boundary condition is the equality of shear force at x = 0 to the inertial resistance of clamp.

In the transform domain these can be written as at x = l

$$\text{Moment } \bar{M} = E^*I \frac{d^2\bar{y}}{dx^2} = 0 \text{ gives}$$

$$\frac{d^2\bar{y}}{dx^2} = 0 \qquad (7)$$

Shear force $V = E^* I \frac{d^3\bar{y}}{dx^3} = 0$ gives

$$\frac{d^3\bar{y}}{dx^3} = 0 \tag{8}$$

At $x = 0$

$$\text{Slope} = \frac{d\bar{y}}{dx} = 0 \tag{9}$$

Similarly, the equality of shear force and the inertial resistance of clamp gives

$$E^* I\left(\frac{d^3\bar{y}}{dx^3}\right) = -M\left(\frac{d^2\bar{y}}{dt^2}\right) = M(i\omega)^2\bar{y} \tag{10}$$

where M is the mass of clamp. The differential equn. in the transform domain becomes

$$\frac{d^4\bar{y}}{dx^4} - \left[\frac{\omega^2 m}{E^* I}\right]\bar{y} = \int_{-\infty}^{\infty} \frac{F_o\, e^{i\omega t}\, \delta(x-0) e^{-i\omega t}\, dt}{E^* I}$$

or

$$\frac{d^4\bar{y}}{dx^4} - \left[\frac{\omega^2 m}{E^* I}\right]\bar{y} = \left[\frac{2\pi}{E^* I}\right] \delta(x-0)\, \delta(\omega-\omega_o) \tag{11}$$

We define k as

$$k^4 = \frac{m\omega^2}{E^* I} \tag{12}$$

$$\frac{d^4\bar{y}}{dx^4} - k^4\bar{y} = \left[\frac{2\pi}{E^* I}\right] \delta(x-0)\, \delta(\omega-\omega_o) \tag{13}$$

The boundary condition in eqn. 10 is rewritten in terms of k as

$$\frac{d^3\bar{y}}{dx^3} = \left(\frac{M}{m}\right) k^4 \bar{y} \quad \text{at } x = 0 \qquad (14)$$

The general homogeneous eqn. corresponding to the problem of eqn. 13 is

$$E^* I \frac{d^4\bar{y}}{dx^4} = k_n^4 \bar{y}_n \qquad (a)$$

whose solution is

$$\bar{y}_n = A_n \operatorname{Sin} k_n x + B_n \operatorname{Cos} k_n x + F_n \operatorname{Sinh} k_n x + G_n \operatorname{Cosh} k_n x \qquad (b)$$

Now, we apply the Boundary Conditions 7 to 10 to obtain

$$-(\operatorname{Cos}\alpha + \operatorname{Cosh}\alpha) A_n + (\operatorname{Sin}\alpha) B_n + \operatorname{Sinh}\alpha\, G_n = 0 \qquad (17)$$

$$(\operatorname{Sin}\alpha + \operatorname{Sinh}\alpha) A_n + \operatorname{Cos}\alpha\, B_n - (\operatorname{Cosh}\alpha) G_n = 0 \qquad (18)$$

$$\alpha\beta A_n + \alpha\beta B_n + \alpha\beta G_n = 0 \qquad (19)$$

where $\beta = \frac{M}{ml}$ (a)

$$\alpha = kl \qquad (b) \qquad (20)$$

For getting non trivial solution for A_n, B_n and G_n we must have

$$\begin{vmatrix} -(\operatorname{Cos}\alpha + \operatorname{Cosh}\alpha) & (\operatorname{Sin}\alpha) & \operatorname{Sinh}\alpha \\ (\operatorname{Sin}\alpha + \operatorname{Sinh}\alpha) & \operatorname{Cos}\alpha & -(\operatorname{Cosh}\alpha) \\ \alpha\beta & \alpha\beta & \alpha\beta \end{vmatrix} = 0 \qquad (21)$$

This sets a condition on α and β such that

$$\alpha\beta = -\frac{(\text{Sin}\alpha)(\text{Cosh}\alpha) + \text{Cos}\alpha\ \text{Sinh}\alpha}{1 + \text{Cos}\alpha\ \text{Cosh}\alpha} \qquad (22)$$

This equn. has theoretically infinite solution for α for given β. Each value of α_n gives a solution $\bar{y}_n$, which after inversion will give the nth mode shape $y_n(x)$ in eqn. 15. This can be derived as a viscoelastic beam of above type.

$$y_n(x) = A_n(\text{Sink}_n x - \text{Sinhk}_n x) + B_n\ \text{Cosk}_n x + G_n \text{Coshk}_n x \qquad (23)$$

where

$$A_n = \frac{(\text{Cos}\alpha_n + \text{Cosh}\alpha_n)}{\left[(\text{Sin}\alpha_n + \text{Sinh}\alpha_n) - (2/\alpha_n\beta)\text{Cos}\alpha_n\right]} G_n \qquad (a)$$

$$B_n = -\frac{\left[\text{Cosh}\alpha_n + (\alpha_n\beta/2)\ (\text{Sin}\alpha_n + \text{Sinh}\alpha_n)\right]}{\left[\text{Cos}\alpha_n - (\frac{\alpha_n\beta}{2})\ (\text{Sin}\alpha_n + \text{Sinh}\alpha_n)\right]} G_n \qquad (b)$$

(24)

Above G_n is unspecified, but is used to normalize $y_n(x)$. Hence we note that one solution of equn. 22 is $\alpha_o = 0$. But if α_o is equal to zero, this would correspond to k = 0 and

$$y_o(x) = B_o + G_o$$

which is constant. This represents a linear translational of motion of the beam in phase with the clamp (no bending).

In order to determine Q_n in eqn. 15, we notice that in the transform domain, it can be written as

$$\bar{y}\ (x,\omega) \ = \ \sum_{n=0}^{\infty} \ y_n(x)\ \bar{Q}_n(\omega) \qquad (25)$$

If this is the complete solution, then it must satisfy the PDE in eqn. 13. Or

$$\sum_{n=0}^{\infty} \frac{d^4\bar{y}_n}{dx^4}\ \bar{Q}_n - k^4 \sum_{n=0}^{\infty} \bar{y}_n\ \bar{Q}_n = \frac{2\pi F_o\ \delta(\omega-\omega_o)\ \delta(x-0)}{E^* I} \qquad (26)$$

Combinin this with the homogeneous equation in eqn. 16a, we get

$$\sum_{n=0}^{\infty} (k_n^4 - k^4)\ \ \bar{y}_n\ \bar{Q}_n = \frac{2\pi F_o\ \delta(\omega-\omega_o)\ \delta(x-0)}{E^* I} \qquad (27)$$

Multiplying this by $y_j(x)$ and integrating from x = 0 to x = l we get

$$\sum_{n=0}^{\infty} (k_n^4 - k^4)\ \ \bar{Q}_n \int_o^l y_n y_j dx = \frac{2\pi F_o\ y_j(o)\delta(\omega-\omega_o)}{E^* I} \qquad (28)$$

We know that the shapes of the modes y_n and y_j are such that

$$\int_o^l y_n(x)\ y_j(x)\ dx = \ - (M/m)\ y_n(o)y_j(o) \qquad (29)$$

$$n \neq j$$

Substituting these in eqn. , we get

$$- \sum_{\substack{n=0 \\ n \neq j}}^{\infty} (k_n^4 - k^4)\ \bar{Q}_n\ y_n(o) + (k_j^4 - k^4)\ \frac{\bar{Q}_j\ m\ k}{M\ y_j(o)}$$

$$= \frac{2\pi F_o m}{ME^* I}\ \delta(\omega - \omega_o) \qquad (30)$$

The relation in eqn.(30) is actually an infinite set of linear simultaneous equations as follows

$$(o - k^4)\ \frac{\bar{Q}_o\ mk}{M\ yo} - (k_1^4 - k^4)\ \bar{Q}_1\ y_1(o)$$

$$- (k_n^4 - k^4)\ \bar{Q}_n\ y_n(o) = \frac{2\pi F_o m}{ME^* I}\ \delta(\omega - \omega_o) \qquad (a)$$

$$- (o - k^4) + (k_1^4 - k^4)\ \frac{Q_1\ mk}{M\ y_1(o)} \quad (k_n^4 - k^4)\ \bar{Q}_n\ y_n(o)$$

$$= \frac{2\pi F_o m}{ME^* I}\ \delta(\omega - \omega_o) \qquad (b)$$

$$(o - k^4)\ \bar{Q}_o\ y_o - (k_1^4 - k^4)\ \bar{Q}_1\ y_1(o)$$

$$(k_n^4 - k^4)\ \frac{Q_n\ mk}{M\ y_n(o)}$$

$$= \frac{2\pi F_o m}{ME^* I}\ \delta(\omega - \omega_o) \qquad (c)$$

Substituting the nth eqn. from eqn. (1) gives the following

$$\bar{Q}_n = \frac{(o - k^4)\ y_o\ [\ (mk/My_o^2) + 1\ ]}{(k_n^4 - k^4)\ y_n(o)\ [\ mk/My_n^2(o)] + 1} \qquad (31)$$

Now we determine $\bar{Q}_o$ since zeroth mode represents the rigidbody motion, this simply means

$$F_o e^{i\omega_o t} = (M + ml) \frac{d^2 y(x,t)}{dt^2} \tag{32}$$

In transform domain this becomes

$$2\pi F_o \delta(\omega - \omega_o) = (M + ml)(i\omega)^2 = M\left(1 + \frac{ml}{M}\right)$$

$$(o - \omega^2)\, y_o\, \bar{Q}_o \tag{33}$$

giving $\bar{Q}_o$ as

$$\bar{Q}_o = \frac{2\pi F_o\, \delta(\omega - \omega_o)}{M\left[(ml/M) + 1\right] y_o\, (o - \omega^2)} \tag{34}$$

On combining eqns. (31) and (34) and inverting gives

$$Q_n(t) = \frac{F_o e^{i\omega_o t}}{M(y_n(o)\left[(\omega_{nr}+i\omega_{ni})^2 - \omega_o^2\right]} \left[1 + \frac{mk}{My_n^2(o)}\right]^{-1}$$

This means that the transverse deflection is given by

$$y(x,t) = \sum_{n=0}^{\infty} \frac{y_n(x) F_o e^{i\omega_o t}}{M(y_n(o)\left[(\omega_{nr}+i\omega_{ni})^2 - \omega_o^2\right]} \left[1 + \frac{mk}{My_n^2(o)}\right]^{-1} \tag{35}$$

$$\therefore \quad \int_o^l y_n^2(x)\, dx = k$$

We find the accelaration from deflection by differentiating it y twice with respect to time as

$$a(x,t) = -\sum_{n=0}^{\infty} \frac{y_n(x)\, F_o \omega_o^2\, e^{i\omega_o t}}{M\, y_n(o) \left[\dfrac{I^2 \alpha_n^8}{l^8 m^2}\right] (E_1+iE_2)^2 - \omega_o^2}$$

$$\times \left[1 + \frac{mk}{My_n^2(o)}\right] \qquad (37)$$

Define

$$\bar{A}(x) = \frac{y_n(x)\, F_o \omega_o^2}{M\, y_n(o) \left[\dfrac{I^2 \alpha_n^8}{l^8 m^2}\right] \left[1 + m \displaystyle\int_o^l \frac{y_n^2(x)\, dx}{My_n^2(o)}\right]}$$

if

$$\bar{B}(x) = \frac{A(x)}{\left(\dfrac{l^8 m^2}{\alpha_n^8 I^2} \omega_o^2 - E_1^2 + E_2^2\right) + 4E_1^2 E_2^2}$$

Then

$$a(x,t) = \sum_{n=0}^{\infty} \bar{B}(x) \left[\frac{l^8 m^2}{\alpha_n^8 I^2} \omega_o^2 - E_1^2 + E_2^2\right) \cos\omega_o t - 2E_1 E_2 \sin\omega_o t\Big]$$

$$+ i \left[\sum_{n=0}^{\infty} \bar{B}(x) \left[\frac{l^8 m^2}{\alpha_n^8 I^2} \omega_o^2 - E_1^2 + E_2^2\right) \sin\omega_o t\right]$$

$$+ 2E_1 E_2 \cos\omega_o t \,]] \qquad (39)$$

If $F = F_o \sin\omega_o t$ then the imagenary part of eqn. (39) will give the $a(x,t)$ as

$$a(x,t) = \sum_{n=0}^{\infty} \bar{B}(x) \left[\frac{l^8 m^2}{\alpha_n^8 I^2} \omega_o^2 - E_1^2 + E_2^2\right) \sin\omega_o t\Big]$$

$$+ 2E_1 E_2 \cos\omega_o t \,]] \qquad (40)$$

$$a(x,t) = \sum_{n=0}^{\infty} B_n(x) \quad Sin(\omega t+\phi) \tag{41}$$

$$a(x,t) = Amp \quad Sin(\omega t+\phi) \tag{42}$$

$$\text{where } \tan\phi = \frac{2E_1E_2}{\left(\frac{\rho_m^2}{\alpha_n^8 I^2} \omega^2 - E_1^2 + E_2^2 \right)} \tag{43}$$

$$\text{Amplitude} = \sum_{n}^{\infty} B_n(x) \tag{44}$$

Now if we know the Amplitude of the accelaration at any two distance x_1 and x_2 from the clamp then we can get values of E_1 & E_2 corresponding to the frequency ω_o.

CHAPTER 3

EXPERIMENTAL SETUP AND PROCEDURE FOR JOINT CHARACTERIZATION

A P.M.M.A. rectangular beam (length 840 mm, width 25.4 mm thickness 5 mm, made with two pieces (300 x 25.4 mm x 5 mm and 540 mm x 25.4 mm x 5 mm) and joined together with diethylene chloride is hung from a fixed iron frame with two threads tied to the ends of the beam. The points of contacts between the thread and the beam and between the thread and the iron frame are rendered immobile with an epoxy glue so as to obviate any friction which might interfere with the ideal propagation of flexural waves in the beam. To generate flexural waves an impact hammer is hung from the iron frame with two threads forming a V shape, the motion of which is restricted to lateral dimensions only, with respect to the beam. Quartz piezotron accelerometers serve to pickup the acceleration response at different points on the beam located on either side of the joint. A multichannel signal coupler conditions the accelerometer response to a degree commensurate with the two F.F.T. nalyzers. A movable support serves to enhance the reproducibility of the impulse force generated by the impact hammer when released from a given height. A small cube of (P.M.M.A.) negligible mass affixed in the middle of beam at the point of impact to make impulse force spatially localized to that point only. An I.B.M. compatible personal Computer (PC-XT) accepts the sampled data transferred from the F.F.T. analyzer through the General Purpose Interface Bus (G.P.I.B.), the pertinent details of

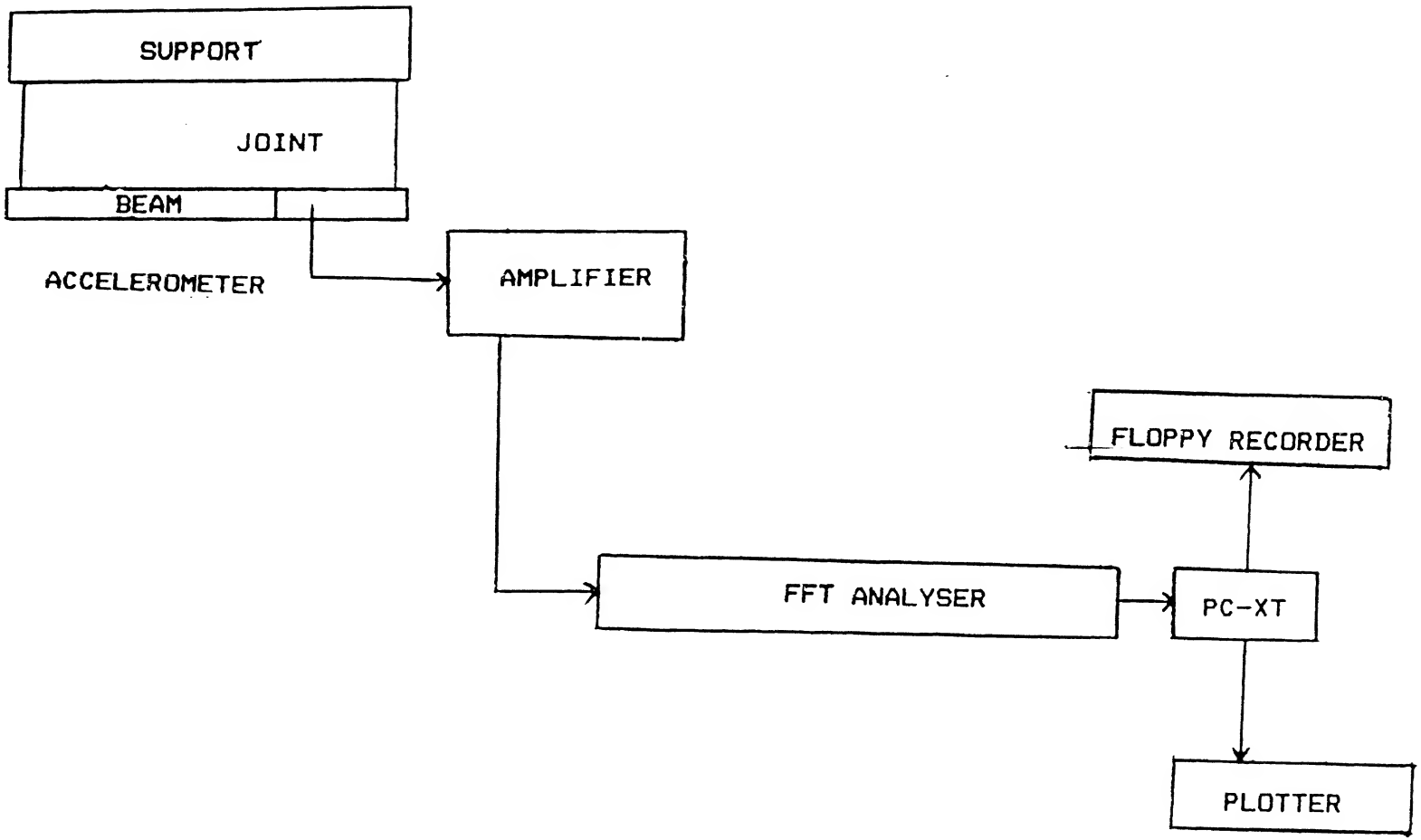

FIG 1 . BLOCK DIAGRAM OF EXPERIMENTAL SET UP

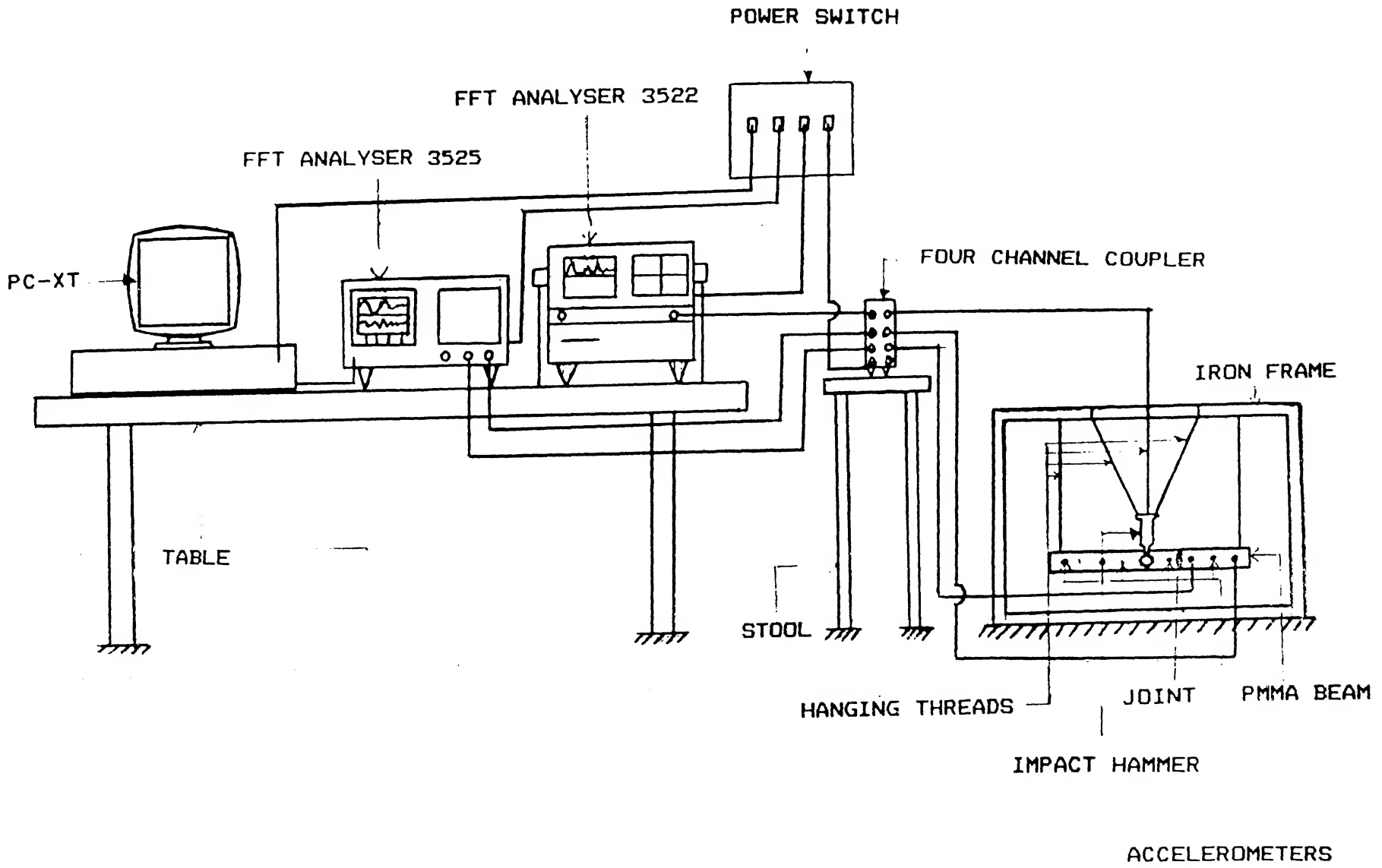

FIG 2 EXPERIMENTAL SET UP FOR JOINT CHARACTERAZATION

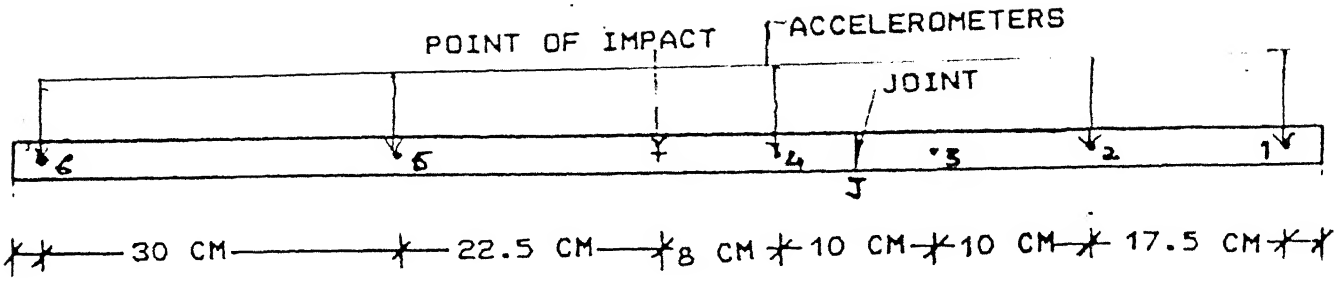

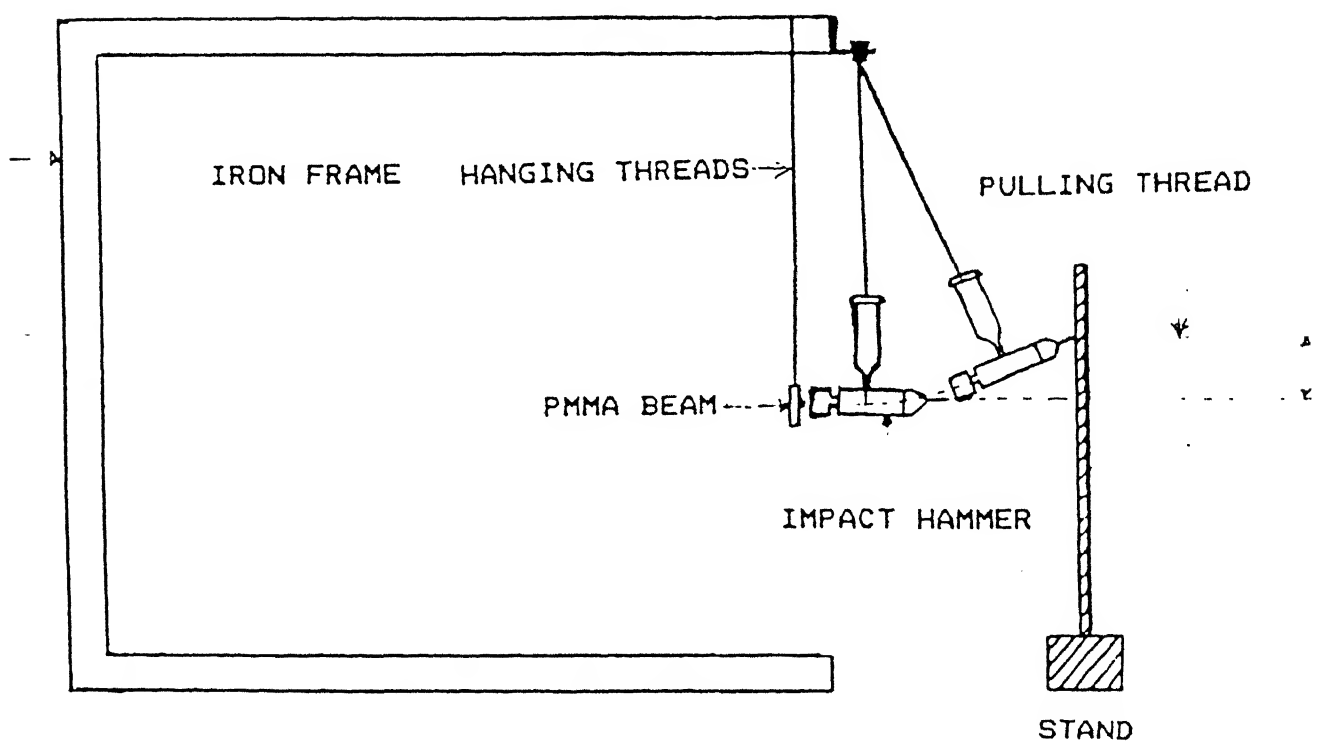

FIG 3 SIDE VIEW OF EXPERIMENTAL SET UP FOR JOINT CHARACTERIZATION

which are provided in Appendix. An application program in Basic interprets the sampled F.F.T. data which is then processed with the P.C.D.S.P. (Personal Computer Digital Signal Processing) software. The application program is given in Appendix 3.

Accelerometer responses at two symmetrical points with respect to impact position are choosen such that one of them lies just before the joint, other one lies symmetrically towards the opposite end. When these two position's responses were compared, we found that after about 0.9 miliseconds their nature changes. This shows that after 0.9 miliseconds of impact the point which is just before joint starts receiving reflected wave from joint, or in 0.9 miliseconds forward wave has travelled from point of impact to the point before joint. Since for about 1 miliseconds the wave is going only in forward direction, therefore we have left data for first 1 milisecond and we have taken F.F.T. of next 4 milisecond data only. W_c have found that this zone contains precious information about the joint characteristic we call this zone as pristine zone.

Procedure

(a) The acceleration responses as well as the impulse force response of the impact hammer at points mentioned in Fig.1 are taken for different joint properties and different hammers.

(b) With the hammer tips of varying softness and for different joints the acceleration response at two points one being 5 cm before joint and another 5 cms. after the joint are stored in F.F.T. analyzer and analyzed. It has been found that lower

frequencies in succession get amplified after the joint while the higher ones in succession get accentuated. For beams with joints of different D.O.P. percentages the amplitude gain that is ratio of amplitude of same frequency before and after the joint were noted and it was found that amplitude gain across the joint of major frequency is a strong monotonically decreasing function of D.O.P. percentage. The major frequency is found to be same before and after the joint. For higher frequencies amplitude gain is more or less one this shows that at higher frequencies joint being very this acts like a solid beam material itself.

CHAPTER 4
EXPERIMENTAL SETUP AND PROCEDURE TO CHARACTERIZE THE MATERIAL

The polymer beam shown in Fig.2 is clamped in the middle and clamping device is connected to the strain gauge based force transducer mounted on the plate, which is connected to shaker head. Force transducer senses force in terms of strains, being caused in strain rossets, mounted in force transducer. The desired frequency is generated by a function generator whose amplitude is amplified by a power amplifier which drives an electromagnetic shaker. The force to which the beam and clamping assembly is subjected is sensed by the load cell (force transducer). The strains caused due to force change the resistance of the strain rossets fitted inside the force transducer. Dynamic force was measured using the force transducer connected to a Q-unit of oscilloscope.

Two piezotron quartz accelerometers are stuck to the beam at distances 15 cm and 30 cm from the clamp, which senses the accelerations at the corresponding points and send the signal to F.F.T. analyzer which displays the time data on the screen. The corresponding acceleration and force from the given voltage on the screen is found by multiplying it with the calibration factors given the corresponding manuals.

Procedure

Desired frequency at which force has to be applied is decided and then that frequency was generated by a function generator and signal was amplified by power amplifier. Then that signal was send to electromagnetic shaker to vibrate it with that frequency. Force

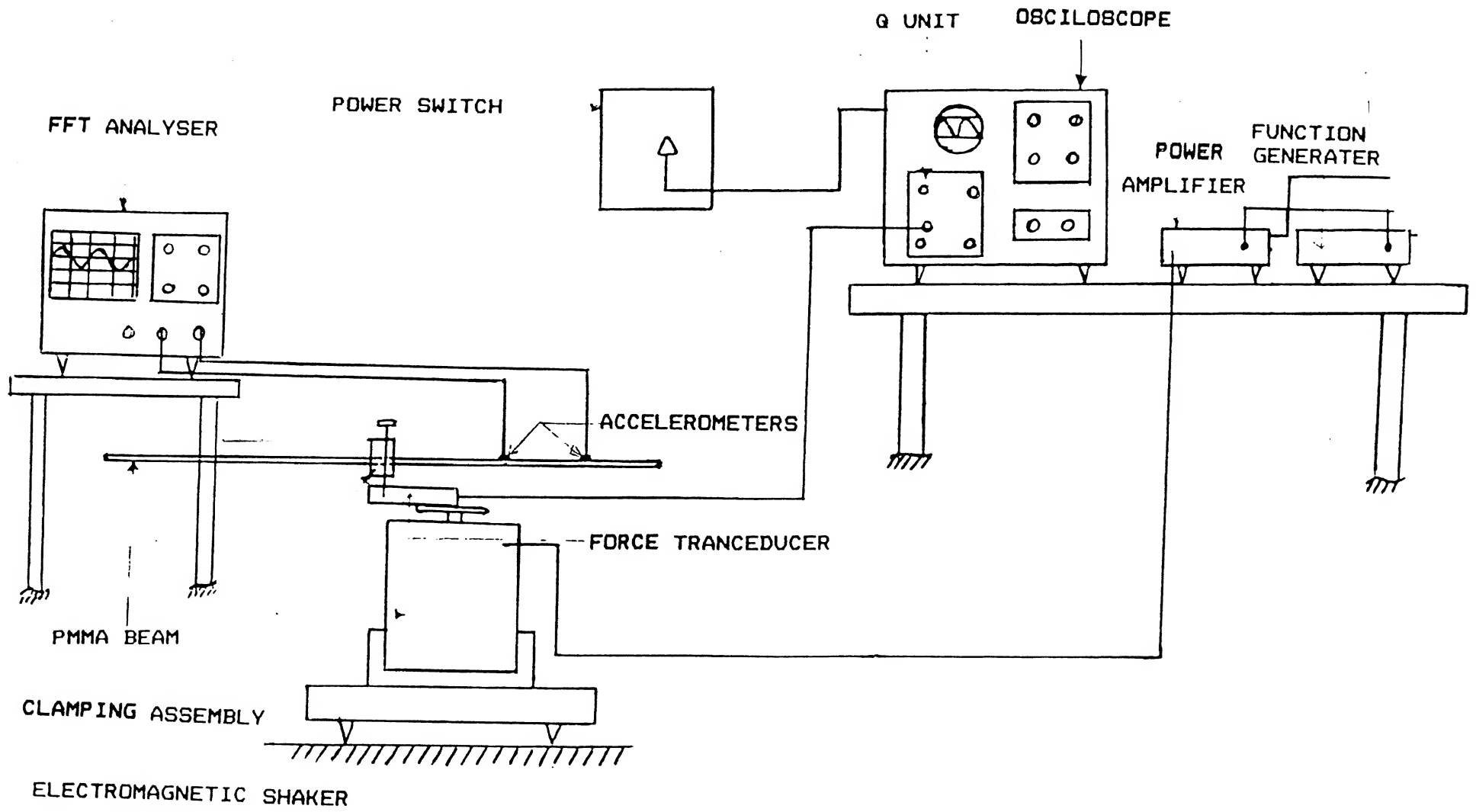

FIG 4 EXPERIMENTAL SET UP FOR MATERIAL CHARACTERIZATION

applied by shaker on load cell as well as clamping device, with beam clamped in it is sensed by load cell and displayed on osciloscope screen as a function of time in terms of milivolts. Since according to analysis shown in chapter 2 for finding out modulus of elasticity for PMMA beam, only amplitude of force is desired therefore we read amplitude of force from screen of osciloscope in terms of milivolts and then this value is multiplied by corresponding calibration factor that is 12.83 $\frac{\text{Newtons}}{mV}$ to get force in Newtons . Similarly accelerometer response was also displayed on F.F.T. analyzers screen in terms of milivolts. Amplitude of acceleration response were read from screen in milivolts and converted in acceleration units (m/sec^2). Now knowing amplitude of force and accelerations at two points and mass of clamp and mass of beam, length, width and size of beam etc. and using the expressions developed in chapter 2 we can find out the complex modulus for given frequency by solving those two nonlinear expressions by iteration. Similar procedure was repeated for different frequencies and corresponding complex modulii were found. Since the equations were simultaneous nonlinear equations they resulted in many solutions. Out of those one solution which was reasonable was

$$E_1 = 5.87 \times 10^{10} \ N/m^2 .$$

$$E_2 = 1.12 \times 10^{8} \ N/m^2$$

This value remained more or less same for higher frequencies say 100, 200 etc. Further higher frequencies could not be generated with our instrument we were not able to get E^* vs frequency relation for P.M.M.A. beam only in frequency range 50 Hz to 250 Hz we were able to find its values.

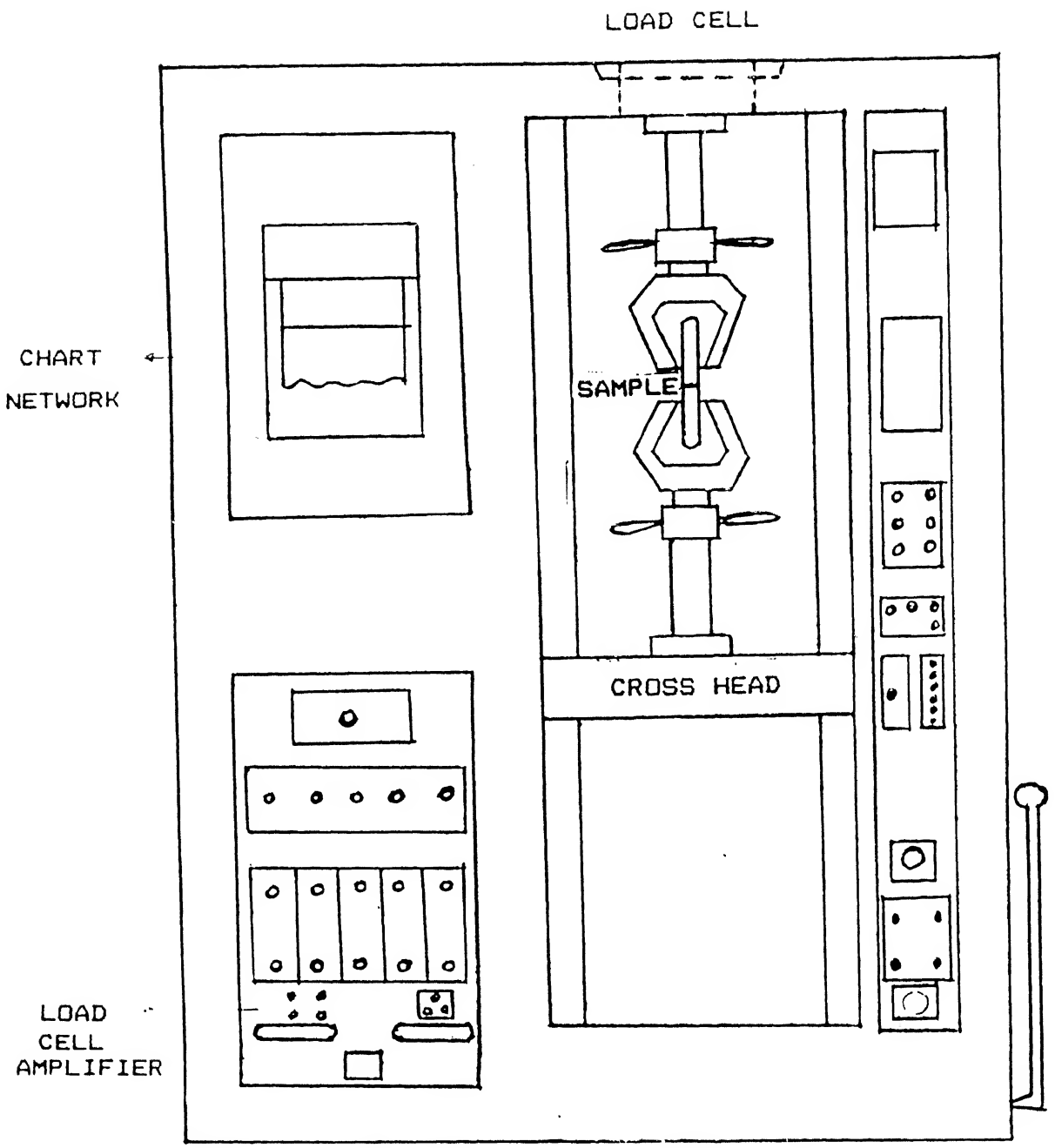

FIG 5 UNIVERSAL TESTING MACHINE (TTCML)

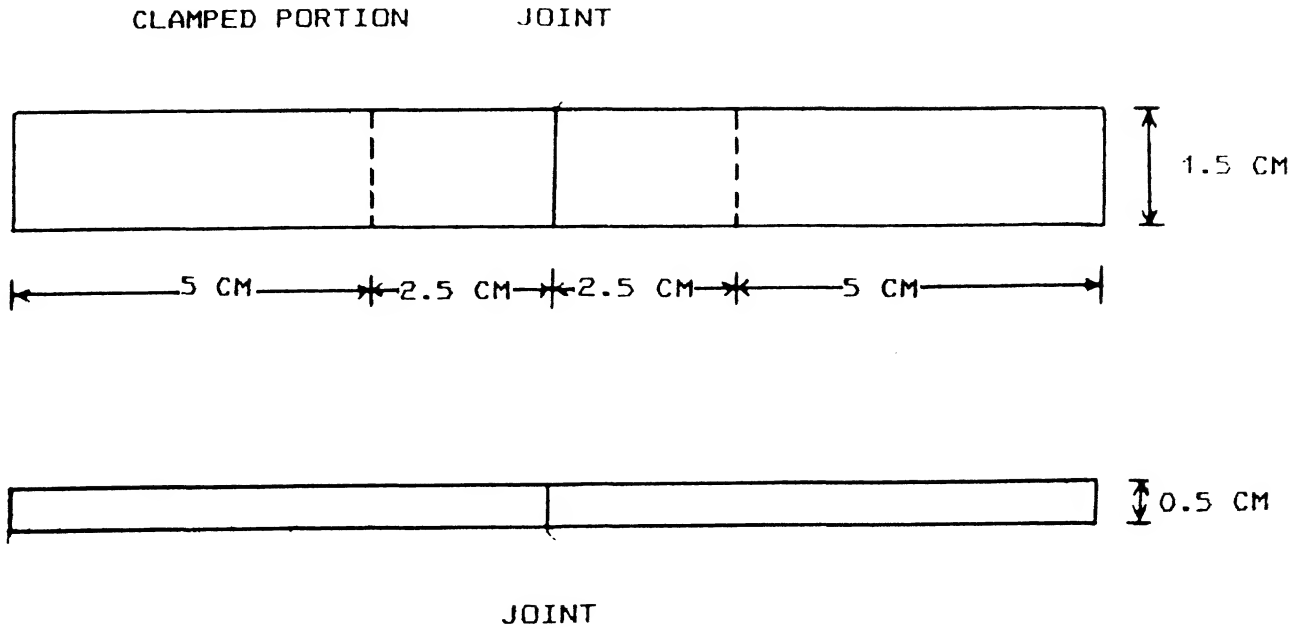

FIG 6 SPECIMEN USED FOR MECHANICAL TESTING

CHAPTER 5

EXPERIMENTAL SETUP AND PROCEDURE FOR ESTIMATING ULTIMATE JOINT STRENGTH

An Universal Testing Machine (U.T.M.) stretches the P.M.M.A. specimen as shown in Fig.3. Specimen is made as per A.S.T.M. standards as shown in Fig.4. Specimens were stretched at slowest possible rate that is at 0.2 mm/min. because specimen is made of viscoelastic material whose modulous of elasticity depends upon rate of loading. Its ultimate strength also depends upon rate of loading. Minimum speed was selected so as to get highest strength. Specimens were stretched till failure. Simultaneously it plots load vs extension curve. Salient features of Testing were

Rate of stretch = 0.2 mm/min.

or cross head speed.

Chart speed = 1 mm/min.

load capacity of machine = 5000 kg

specimens were 15 mm wide and 5 mm thick. Because jaw of machine cannot accomodate width more than 25 mm and thickness more than 12.5 mm.

Procedure

For specimens with different D.O.P. percentage stress taken at the time of failure was computed and averaged over fine samples of same specimen. The ultimate strength is found to be a strong monotonically decreasing function of D.O.P. percentage.

Experimental Data

at ω_o = 60 Hz (P.A. = Peak Amplitude)

at .15 P.A. = 327.544 mV

at .30 P.A. = 709.679 mV

at ω_o = 30 Hz

at .15 P.A. = 3.25906 V

at .30 P.A. = 1.04814 V

at ω_o = 300 Hz

at .15 P.A. = 1.33201 V

at .30 P.A. = 600.498 mV

at ω_o = 100 Hz

at .15 P.A. = 2.38561 V

at .30 P.A. = 1.5886 V

at ω_o = 200 Hz

at .15 P.A. = 595.039 mV

at .30 P.A. = 185.609 mV

Computational work for calculation of E_1 & E_2

CHAPTER 6

Results and Discussion

The Joints in a primary structure could be mechanical welded or adhesive in nature. In this work we focus our attention on the adhesive joints in polymer beams. The polymer consist of large molecules which may have linear or cross linked chains. The latter are network in structure where all polymer molecules are linked together giving a giant molecule. The difference between the linear and network molecules lies in their solubility in that the latter does not dissolve but incorporate solvent into themselves through swelling.

When we wish to prepare joints in polymeric beams, we have only the following limited options.

1. Use a suitable adhesive which sticks the two adherends.
2. Use a solvent system which disolves the material of adherends and its evaporation leaves behind a joint.

In any given polymer structure (as shown in figure 4) the chain ends of polymer molecule are dangling out when we apply an adhesive the polymer chain ends must unentangle and penetrate into the adhesive and the driving force for this is obtained by the favourable difference in their chemical potentials. This inaterpenetration gives rise to two interfaces as shown. In contrast to this, when a solvent is used the chain ends of the two adherends must dissolve into the solvent and interpenetrate into each other. On evaporation of the solvent, this leads to single interface. The strength of the joint arises because of this interpenetration of chain endseither into each other or into the adhesive. The complex combination of the strength of the adhesive

and that of the interpenetration of the polymer chains is not yet understood very well and the purpose of this study is to throw some light upon this.

In this study we have chosen a beam made of Polymethylmethacrylate (PMMA) and we have cut it at a suitable location. The two pieces of the adherends are joined using Ethylenedichloride solvent. This has very high vapour pressure and gives an excellent joint. In order to vary the property of this joint we have mixed Dioctylphthlate (DOP), a plasticizer, (C_6H_4 - 1,2 - [CO_2 CH_2 CH (C_2H_5) (CH_2)$_3$ CH_3]$_2$ with it while making the joint. The result of this way of joining is that the solvent evaporates with DOP remaining within a very thin layer around the interface. It is desired now to determine the changes of the viscoelastic properties of this interface.

For determining the properties of the interface we have employed the use of transverse flexural waves generated through impacting. We strike a beam with a small metallic bob by swinging it from a known height it generates flexural waves on impacting which travels both ways with equal likelihood as shown in Fig.5. Let us say we decide to measure acceleration at point A using a suitable accelerometer. The forward wave from the point of impact travels to this point first. After it has travelled across and reached point of joint J, some of it is reflected and the remaineder is transmitted through it. This is reflected from the end of the beam B passes through the joint once again and ultimately reaches the point of measurement. Similarly energy travelling towards C is also reflected in due course and reaches point A. Since the waves take a finite amount of time to travel, it is expected that these reach point A at different time and this

way produces a separation between these. This separation is not expected to be clearcut, since higher frequency waves travel faster and may overlap with other waves. However, it appears possible to distinguish the various regions.

Figure 7 shows the pristive time zone. The F.F.T. of which carries the desire information about the viscoelastic properties of the interface which acts as a natural band limited filter modifying the elemental frequencies.

Figure 7 shows acceleration response before joint in time domain and Figure 8 shows acceleration response after joint in time domain. Figure 9 and Figure 10 show F.F.T. of acceleration response before and after joint. Figure 11 shows amplitude of dominant frequency vs different locations on the beam.

A drop of eighty percentage in amplitude gain of the major frequency of 2517 radians per second, shown in figure 12,when D.O.P. percentage in the joint is varied from 0 to 20, reflects strong relation between the amplitude gain and the viscoelasticity of the joint.

With linear regression the following first order model fits approximately, the experimental data.

$$y_1 = 25 - x \tag{45}$$

where

y_1 = amplitude gain;

x = % DOP.

The relationship between ultimate strength and percentage D.O.P. is modelled with the following first order polynomial approximately by

$$y_2 = 250 - 10\,x \tag{46}$$

Fig 7 Acceleration Response

Before Joint

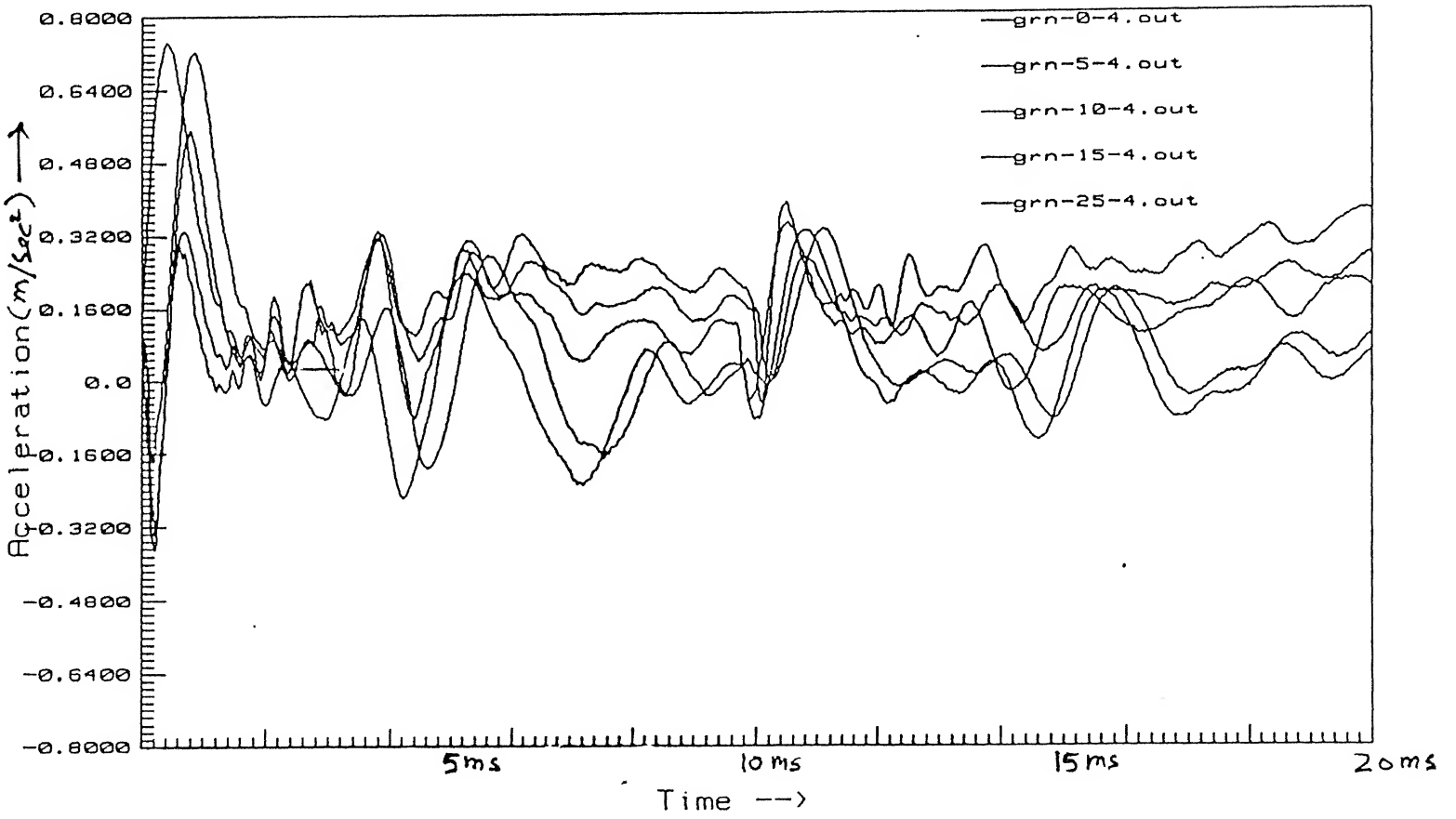

Fig 8 Acceleration Response

After Joint

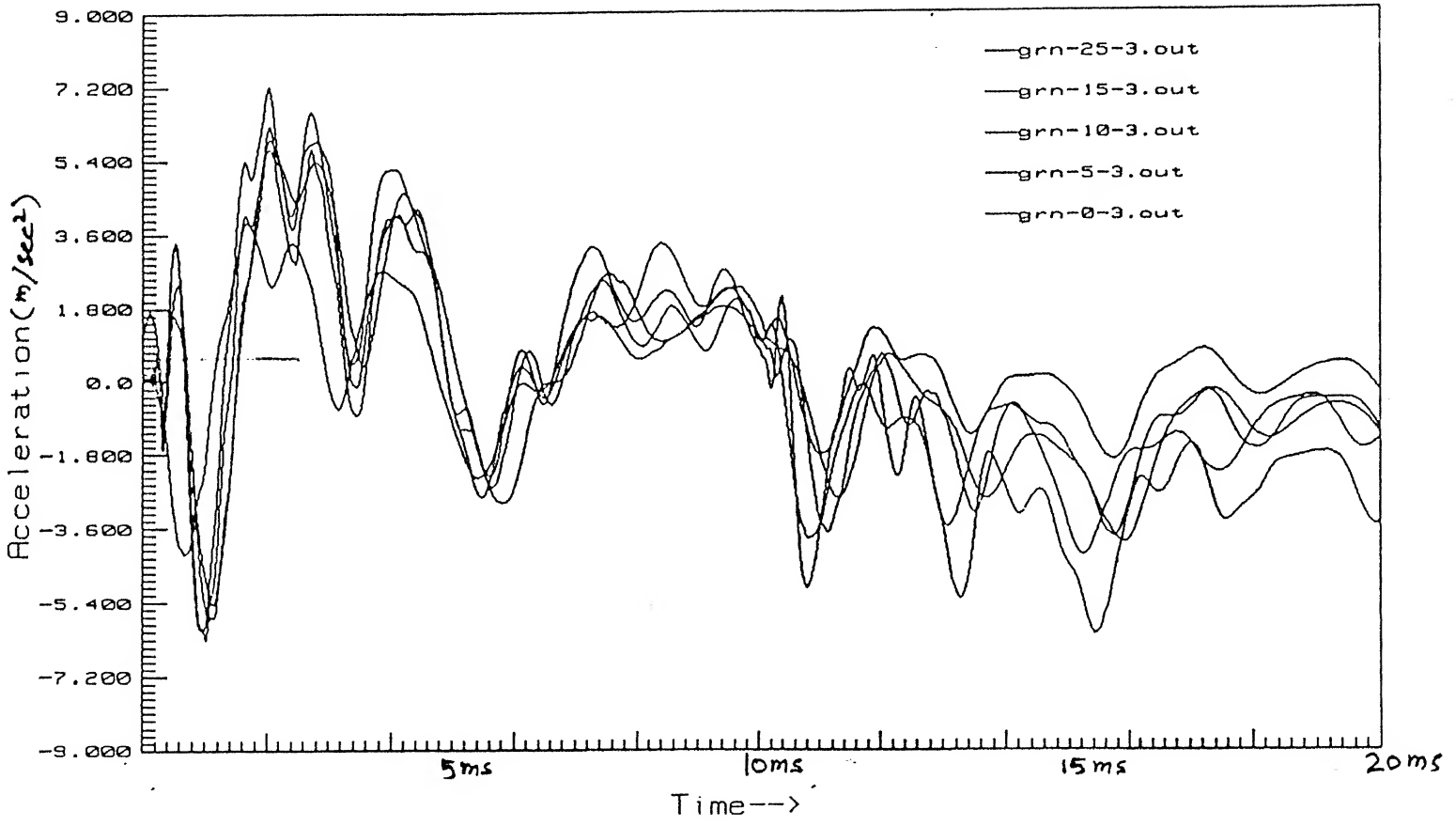

Fig 9 fft_of_accn_response

before joint

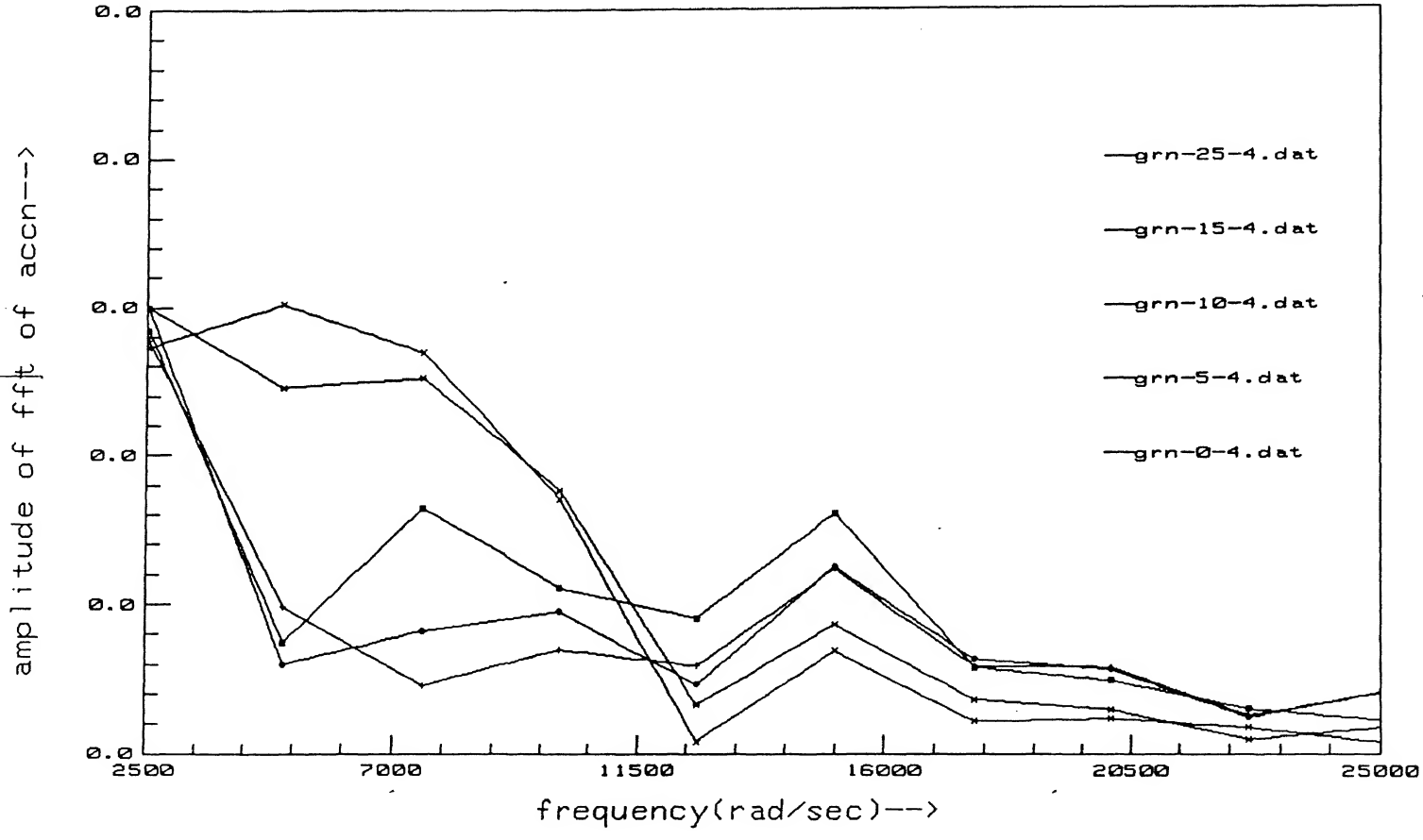

Fig 10 fft_of_accn_response

after joint

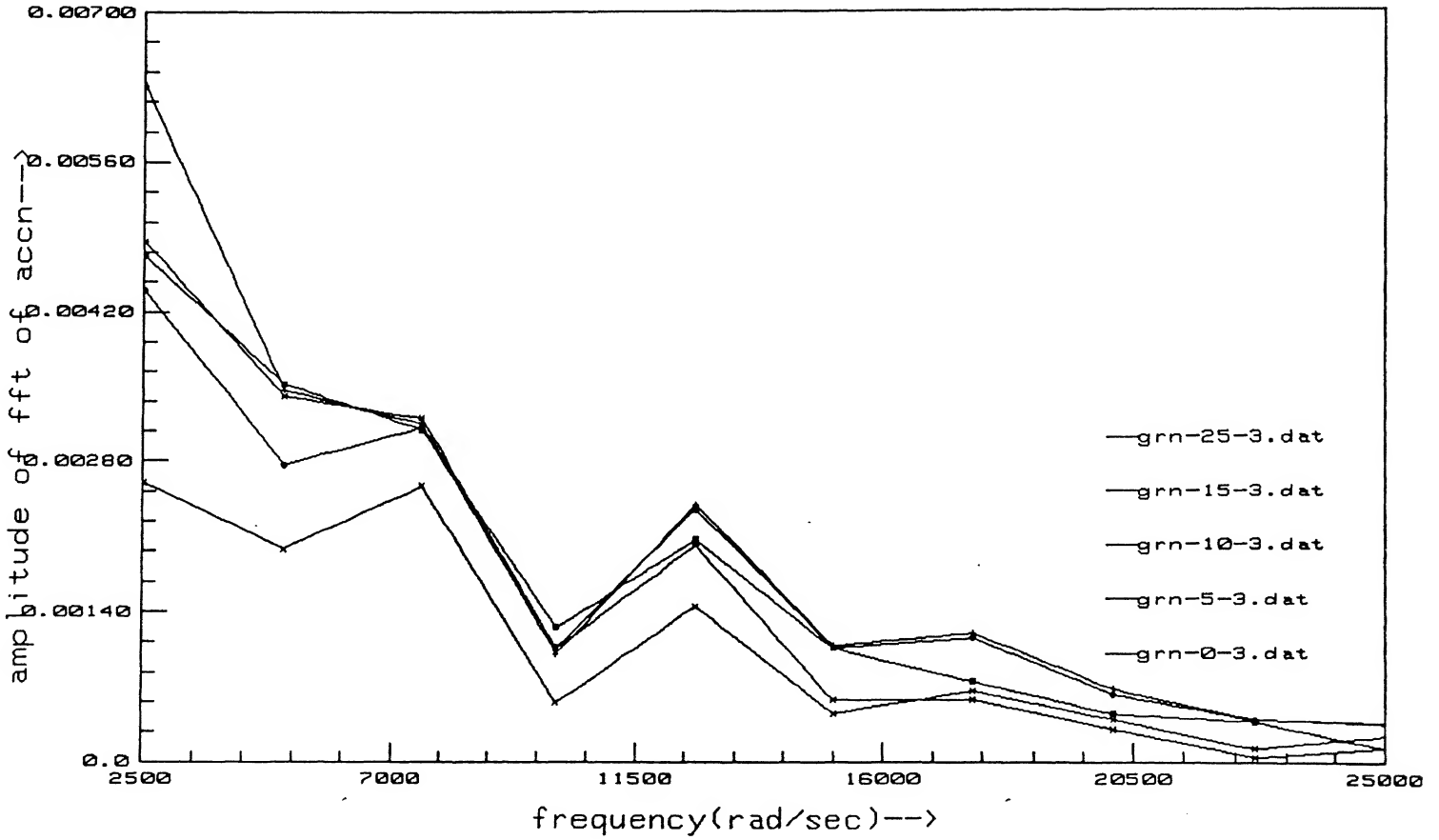

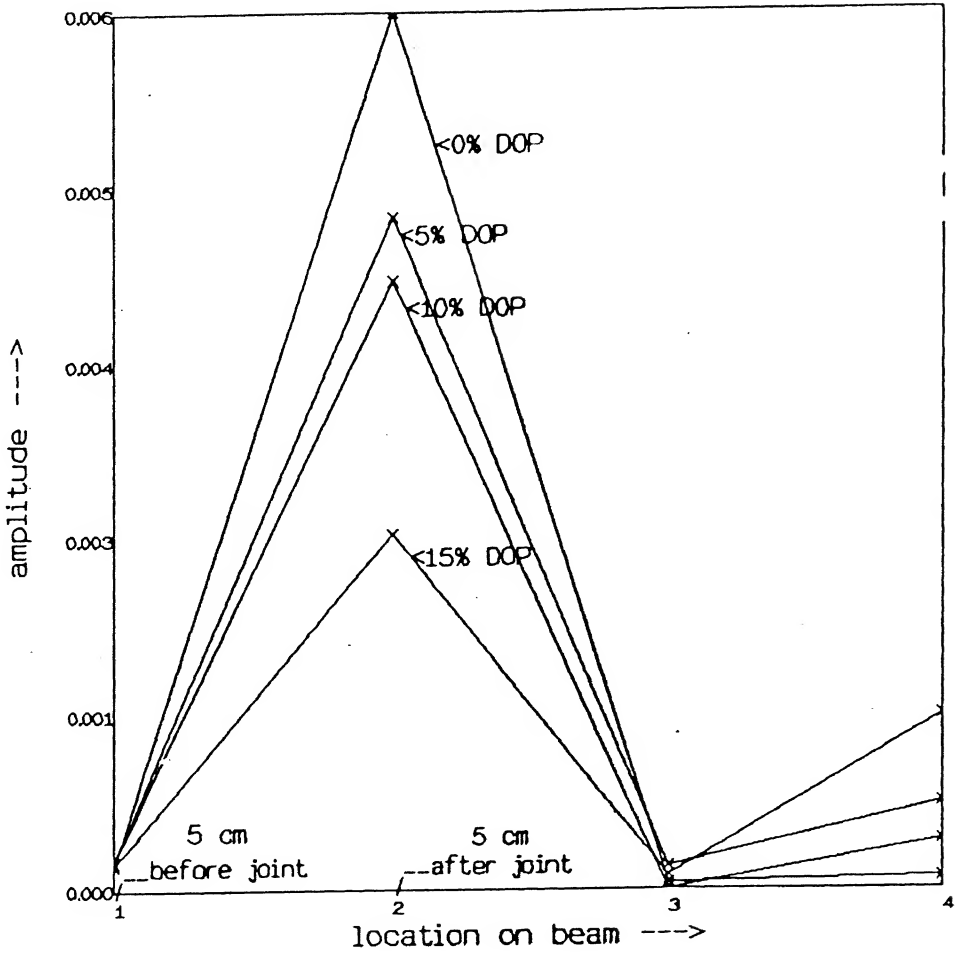

FIG 11 AMPLITUDE OF MAJOR FREQUENCY IN 1 TO 5 MILLI SECOND TIME RANGE VS DIFFERENT LOCATIONS ON THE BEAM (FOR VARIOUS % OF DOP)

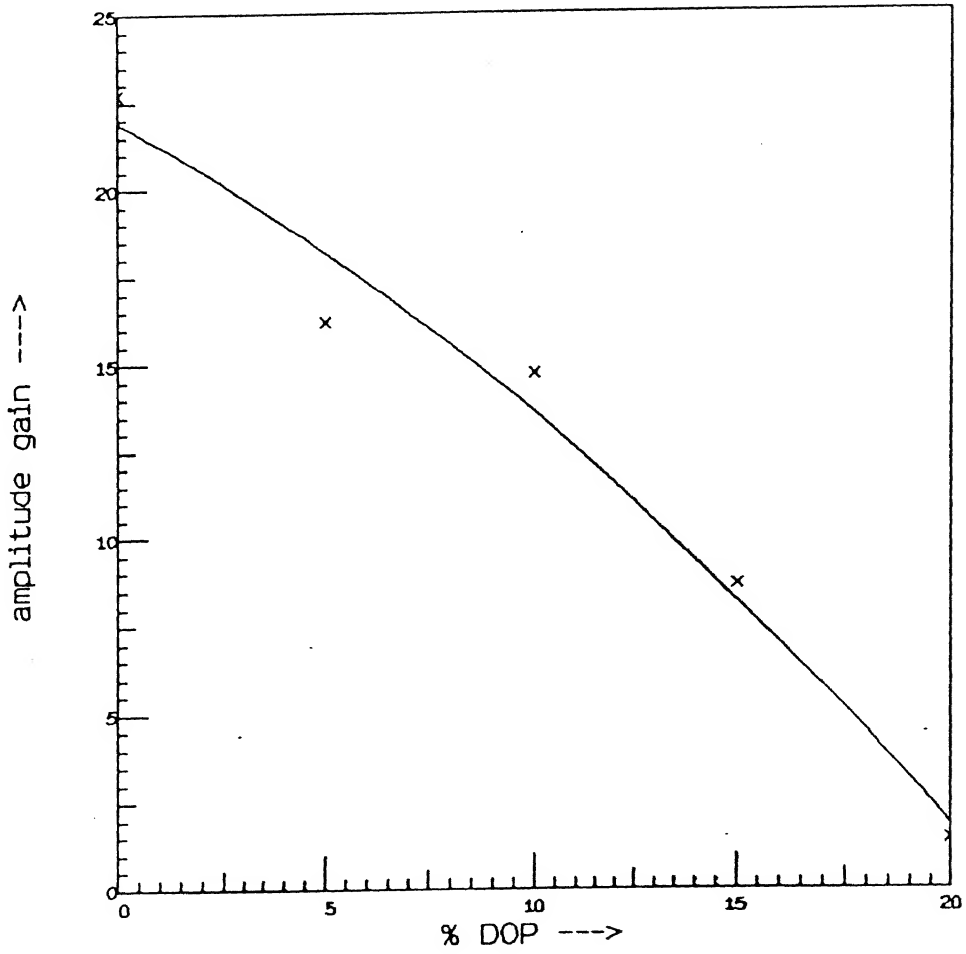

FIG 12 AMPLITUDE GAIN OF MAJOR FREQUENCY BEFORE AND AFTER JOINT

FOR FIRST 1TO 5 MILLI SECOND TIME DATA

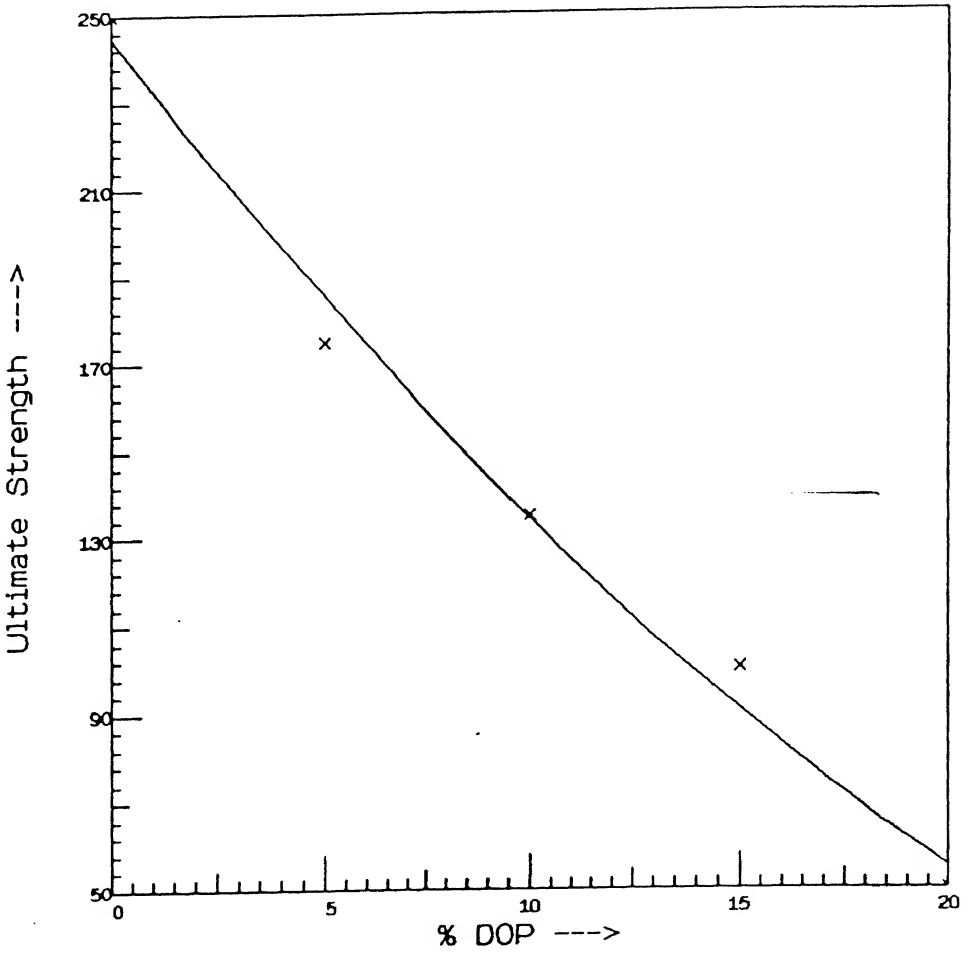

FIG 13 ULTIMATE STRENGTH OF VISCOELASTIC JOINT VS PLASTICIZER CONTENT IN IT

y_2 = ultimate strength of joint;

x = % DOP.

Eliminating percentage D.O.P. we get, by solving the above two equations, the following relationship between ultimate strength of joint and the amplitude gain of the major frequency of the pristive zone.

$$y_2 = 10\ y_1 \text{ (approximately)} \qquad (47)$$

where

y_2 = ultimate strength;

y_1 = amplitude gain

CHAPTER 7

Conclusions

We observe that the strength of adhesive joint consists of a complex combination of the strength of the adhesive layer and that of the two interfacial regions. It is possible to study the strength of the adhesive material independently, but very few studies are reported concerning the interfacial region of the joint. We have chosen to study a beam of polymethyl methacrylate (PMMA) and joints made in it by using ethylene dichloride as a solvent. The thickness of this joint is negligible and can be assumed to consist of only interfacial region. We have chosen to vary its property by using dioctyl phthalate (DOP) plasticizer and wish to study its effect upon the flexural wave propagation through it.

We observe the following :

1. The flexural wave generated across the joint through impacting carries information about the joint while getting transmitted.
2. Joint interface acts as a natural band limited filter.
3. The frequencies across the joint are preserved while their amplitude gets modified.
4. The amplitude of the major frequency of the prestive zone gets amplified.
5. This amplitude gain is strongly correlated to the viscoelastic properly of the joint.
6. The equation $\gamma_2 = |o\gamma_1$ can be successfully used for the non destructive testing of the joint. (γ_2 = ultimate strength, γ_1 = % amplitude gain)

REFERENCES

1. R.B. Thompson and D.O. Thompson, Past Experience in the Development of Tests for Adhesive Bond Strength, *J. Adhesion Sci. Technol.*, 5, 583 (1991).
2. D. Jian and L. Rose, An Ultrasonic Interface Layer Model for Bond Evaluation, *J. Adhesion Sci. Technol.*, 5, 631 (1991).
3. S.E. Hanneman and V.K. Kinra, A New Technique for Ultrasonic Nondestructive Evaluation of Adhesive Joints, Part-I, Theory, *Experimental Mechanics*, 323, Dec. (1992).
4. S.E. Hanneman and V.K. Kinra, A New Technique for Ultrasonic Nondestructive Evaluation of Adhesive Joints, Part-II, Experimental, *Experimental Mechanics*, 332, Dec. (1992).
5. A. Tiwari, G. Henneke, II and J.C. Duke, Acousto-Ultrasonic (AU) Technique for Assuming Adhesive Bond Quality, *J. of Adhesion*, 34, 1 (1991).
6. H.L. Groth, Viscoelastic and Viscoplastic Stress Analysis of Adhesive Joints, *Int. J. Adhesion and Adhesives*, 10, 207, July (1990).
7. Aleksander Pilarski and Joseph L. Rose, A Transverse-Wave Ultrasonic Oblique-incidence Technique for Interfacial Weakness Detection in Adhesive Bonds, *J. App. Phys.*, 63, 2, Jan. (1988).
8. H. Ishikawa, R. Yuuki, N.Y. Chung and S. Nakano, Mixed Mode Fracture Criteria on Adhesive Joints, Mixed Mode Fracture and Fatigue, 221, July 15-19, Vienna, Austria.
9. M.M. Ratwani, H.P. Kan and D.D. Liu, Time Dependent Adhesive Behavior Effects in a Stepped Lap Joint, American Institute of Aeronautics and Astronautics 248, (1981).

10. M.D. Rao and M.J. Crocker, Analytical and Experimental Study of the Vibration of Bonded Beams with a Lap Joint, Transections of the ASME, 112, 444, Oct. (1992).

11. S.A. Hashim, M.J. Carvling and T.E. Winkle, Design and Assessment Methodologies for Adhesively Bonded Structural Connections, *Int. J. Adhesion and Adhesives*, 10, 139, July, (1991).

12. D.A. Bigwood and A.D. Crocombe, Nonlinear Adhesive Bonded Joints Design Analysis, *Int. J. Adhesion and Adhesives*, 10, 31, Jan. (1990).

13. D.A. Bigwood and A.D. Crocombe, Elastic Analysis and Engineering Design Formulae for Bonded Joints, *Int. J. Adhesion and Adhesives*, 10, 339, Jan. (1990).

14. H.L. Growth and J. Brottare, Evaluation of Singular Intensity Factors in Elastic-Plastic Materials, *Journal of Testing and Evaluation*, 291, May (1988).

15. A Needleman, Analysis of Interfacial Failure, *Appl. Mech. Rev.*, 43, 5274, Part 2, May (1990).

16. Z. Suo, Failure of Brittle Adhesive Joints, *Appl. Mech. Rev.*, 43, 5276, Part 2, May (1990).

17. Steen Krenk, Energy Release Rate of Symmetric Adhesive Joints, *Engineering Fracture Mechanics*, 43, 549 (1992).

18. T. Sawa, H. Ishikawa and K. Muto, The Strength of Joints Combining Adhesives with Bolts, ISME, *Int. J. Series I*, 35, 38, (1992).

19. K.C. Kairouz, F.L. Mathews, Mechanism of Failure in Bonded CFRP Single Loop Joints with Different Stacking Sequences, Proc. of the Inst. of Mech. Engg., 47, (1990).

20. J.P. Jeandrau, Intrinsic Mechanical Characterization of Structural Adhesives, *Int. J. Adhesion and Adhesives*, 6, 229, Oct. (1986).

21. Robert, D. Adams, Strength Prediction for Lap Joints, Especially with Composite Adherends, A Review, *Int. J. Adhesion and Adhesives*, 6, 219, Oct. (1986).

22. A.A. Khalil and M.R. Bayoumi, Effect of Loading Rate on Fracture Toughness of Bonded Joints, *Int. J. Adhesion and Adhesives*, 11, 25, Jan. (1991).

23. F. Edde and Y. Verreman, On the Fracture Parameters in a Clamped Cracked Lap Shear Adhesive Joint, *Int. J. Adhesion and Adhesives*, 12, 43, Jan. (1992).

24. T. Hattori, S. Sakata, G. Murakami, A Stress Singularity Parameter Approach for Evaluating the Interfacial Reliability of Plastic Encapsulated LSI Devices, *J. of Eloelectronic Packing*, 111, 243, Dec. (1989).

25. R. Davis and A.A. Khalil, Design and Analysis of Bonded Double Containment Corner Joints, *Int. J. Adhesion and Adhesives*, 10, 25, Jan. (1990).

26. T.S. Ramamurthy and A.K. Rao, Analysis of Bonded Joints with Arbitrary Adherend Shapes and Adhesive Non-limearities, *Journal of Aro. Soc. of India*, 36, 29, (1983).

27. Du Chen and Shun Cheng, An Analysis of Adhesive Bonded Single Lap Joints, *J. of Appl. Mech.*, 105, 109, March (1983).

28. J.P. Jeandrau, Analysis and Design of Adhesive Bonded Structural Joints : New Tools for Engineers, Mechanical Behaviour of Adhesive Joints, 493 (1987).

29. G. Fernlund and J.K. Spelt, Analytical Method for Calculating Adhesive Joint Fracture Parameters, *Engineering Fracture Mechanics*, 40, 119 (1991).

30. G. Fernlund and J.K. Spelt, Failure Load Prediction of Structural Adhesive Joints, *Int. J. Adhesion and Adhesives*, 11, 213, Oct. (1991).

31. Xiaying Mu and Hurang Hu, A Finite Element Elastic-Plastic -creep Analysis of Materials with Temperature Dependent Properties, *Computers & Structures*, 30, 953 (1988).

32. H.L. Groth, Calculating of Stress in Bonded Joints Using The Substructuring Technique, *Int. J. Adhesion and Adhesives*, 6, 31, Jan. (1986).

33. Y. Yamada, N. Yoshimura and T. Sakurai, Plastic Stress Strain Matrix and Its Application for the Solution of Elastic Plastic Problems by the Finite Element Method, *Int. J. Mech. Sci.*, 10, 343 (1968).

34. Had J., Rabah Y., Aivazzadehs Verchery G., Edge Effects Analysis and Influence of Defects in Adhesively Bonded Composite Joints Using Interface Finite Elements, American Society for Testing and Materials, (1986).

35. S. Aivazzadeh, B. Bichara, A. Ghazal and G. Verehery, Special Mixed Finite Elements for Interfacial Stress Analysis of Adhesively Bonded Joints, Adhesively Bonded Joint Testing, Analysis and Design, ASTM, STP 981.

36. S.S. Aivazzadeh, M. Babi, G. Verehery, Assessment and Comparison of Classical, Mixed and Interface Elements for the Stress Analysis in Adhesive Joints, Mechanical Behaviour of Adhesive Joints, 537 (1987).

37. W.S. Johnson, Stress Analysis of the Cracked-Lap-Shear Specimen : An ASTM Round-Robin, J. of Testing and Evaluation, TTEVA, 15, 302 (1987).

38. T. Sarva, K. Temma and Y. Isunoda, Axisymmetric Stress Analysis of Adhesive butt Joints of Dissimilar Solid Cylinders Subjected to External Tensile Loads, *Int. J. Adhesion and Adhesives*, 9, 161, July (1989).

39. K. Temma, T. Sawa and A. Iwata, Two Dimensional Stress Analysis of Adhesive butt Joints Subjected to Cleavag Loads, *Int. J. Adhesion and Adhesives*, 10, 285, Oct. (1990).

40. P. Czarnocki and K. Piekarski, Non Linear Numerical Stress Analysis of a Symmetric Adhesive Bonded Lap Joints, *Int. J. Adhesion and Adhesives*, 6, 157 (1986).

41. K. Temma, T. Sawa, and Y. Tsunoda, Three Dimensional Stress Analysis of Adhesive butt Joints with Disbonded Areas and Spew Fillets, *Int. J. Adhesion and Adhesives*, 10, 294, (1990).

42. H.L. Growth and P. Nordlund, Shape Optimization of Bonded Joints, *Int. J. Adhesion and Adhesives*, 11, 204, Oct. (1991).

43. S. Marcolefas, V. Kostopoulos and S.A. Paipetis, Nonlinear Analysis of a Metal to Composite Scorf Joint, *Int. J. of Mech. Sci.*, 33, 961 (1991).

44. J.P. Jeandrau, Analysis and Design Data for Adhesively Bonded Joints, *Int. J. Adhesion and Adhesives*, 11, 71, April (1991).

45. K. Temma, T. Sewa and A. Iwata, Two Dimensional Stress Analysis of Adhesive butt Joints subjected to Cleavage Loads, *Int. J. Adhesion and Adhesives*, 298, Oct. (1990).

46. K. Temma, T. Sawa and T. Tsunoda, Three Dimensional Stress Analysis of Adhesive butt Joints with Disbonded Areas and Spew Fillets, *Int. J. Adhesion and Adhesives*, 168, July (1989).

47. Yaowu Liu and Kuan Chen, A Two-dimensional Mesh-generator and Variable Order Triangular and Rectangular Elements, *Computers and Structures*, 29, 161, 1033 (1988).

48. T. Sawa, K. Temma, H. Ishikawa, Three-dimensional Stress Analysis of Adhesive Butt Joints of Solid Cylinders Subjected to External Tensile Loads, *J. Adhesion*, 31, 33 (1989).

49. Du Chen, Shun Cheng, Stress Distribution in Plane Scarf and Butt Joints, Transactions of ASME, 57, March (1990), *J. of Appl. Mech.*, 57, 78, March (1990).

50. Phillip G. Wapner and W.C. Forsman, Fourier Transform method in Linear Viscoelastic Analysis, The vibrating Viscoelastic Reed, Transactions of Society of Rheology 15 : 4, 603 - 626 (1971).

APPENDIX 1

SPECTRAL ANALYSIS

Several analytical techniques exist in the literature for the analysis of wave propagation problems. Central among these is the method of Fourier Transform analysis which is also sometimes called as spectral analysis. In this, any given signal is assumed to be formed by a superposition of many infinitely long wave trains of different frequencies. In the following we describe this in brief.

CONTINUOUS FOURIER TRANSFORM

The continuous fourier transform of a function F(t) is defined in the time domain $-\infty$ to $+\infty$ as

$$C(\omega) = \int_{-\infty}^{+\infty} F(t)\, e^{-i\omega t}\, dt \qquad (a)$$

$$2\pi\, F(t) = \int_{-\infty}^{+\infty} C(\omega)\, e^{-i\omega t}\, dw \qquad (b) \quad (1.1)$$

Above $C(\omega)$ is a continuous fourier transform, ω is the angular frequency and i is complex number equal to $\sqrt{-1}$. Eqn. 1(b) shows inverse transform and 1(a) shows forward transform. This arbitrary convention arises because the signal to be transformed are usually available in the time domain. The factor 2π is for sequential recovery of forward as well as backward or inverse transform for the original signal. Using frequency relation $2\pi f = \omega$, we get

$$C(f) = \int_{-\infty}^{+\infty} F(t)\, e^{-i2\pi ft}\, dt \qquad (a)$$

$$F(t) = \int_{-\infty}^{+\infty} C^{*}(f)\, e^{-i2\pi ft}\, df \qquad (b) \quad (1.2)$$

where the superscript * refers to the fact that the variables are complex conjugate. Some of the properties of Fourier Transforms are listed in Table A1.

REAL TIME FUNCTIONS

The following transform pairs are valid

$$Fe(t) \leftrightarrow 1/2\ [\ C(\omega) + C(-\omega)\ ] = \text{Real}\ [C(\omega)]$$

$$Fo(t) \leftrightarrow 1/2\ [\ C(\omega) + C(-\omega)\ ] = i\ \text{Image}\ [C(\omega)]$$

for both F(t) and C(ω) being complex. In practice the functions of usual interest in wave analysis are when F(t) is real. To see the effect of this, Eqns. are rewritten in terms of real (C_R) and imaginary parts (C_i) of C in terms of F_R and F_I of F as

$$2\pi F_R = \int [C_R \cos(\omega t) - C_I \sin(\omega t)]\, dw \qquad (a)$$

$$C_R = \int [F_R \cos(\omega t) - F_I \sin(\omega t)]\, dt \qquad (b)$$

$$2\pi F_I = \int [C_R \sin(\omega t) - C_I \cos(\omega t)]\, dw \qquad (c)$$

$$C_R = \int [F_R \sin(\omega t) - F_I \cos(\omega t)]\, dt \qquad (d) \quad (1.3)$$

Using the following decomposition

$$\cos\theta = (1/2)\ [\ e^{i\theta} + e^{-i\theta}\ ] \text{ and} \qquad (a)$$

$$\sin\theta = -i\ (1/2)\ [\ e^{i\theta} + e^{-i\theta}\ ] \qquad (b) \quad (1.4)$$

If F(t) is real only, C_R is even and C_I is odd mathematically

$$C_R(-\omega) = C_R(\omega), \quad C_I(-\omega) = -C_I(\omega) \tag{1.5}$$

which says that the functions are symmetrical and asymmetrical, respectively about the zero frequency point. This can also be expressed as saying that the negative frequency side of the transform is the complex conjugate of the positive side and is written as

$$C(-\omega) = C^*(-\omega) \tag{1.6}$$

FOURIER SERIES

A fourier series representation of a function assumes the function as periodic in the time domain. Consequently, it can only be an approximation to the transient function found in wave analysis since these are assumed to be present on the full domain. In elementary terms, if the signal has large duration of zero amplitude and the analysis assumes it repeats itself on a period very large compared to the time of interest of the wave, then for all intents and purposes it behaves as an infinite wave.

BASIC REPRESENTATION

A function F(t) with period T can be expressed in the form of a Fourier series as

$$F(t) = 1/2\ a_o + \sum_{n=1}^{\infty} \left[a_n \operatorname{Cos}\left(2\pi n \frac{t}{T} \right) + b_n \operatorname{Sin}\left(2\pi n \frac{t}{T} \right) \right] \tag{1.7}$$

where the coefficient are obtained from

$$a_n = \frac{2}{T} \int_o^T F(t) \text{ Cos } (2\pi n\ t/T)\ dt, \quad n = 0,1,2,.... \quad (a)$$

$$b_n = \frac{2}{T} \int_o^T F(t) \text{ Sin } (2\pi n\ t/T)\ dt, \quad n = 1,2,.... \quad (a) \quad (1.8)$$

In these n can take on positive as well as negative values. It is apparent that a_n is symmetric while b_n is antisymmetric about n = 0. Using the identities of Table A1 and introducing in terms of discrete frequency $\omega_n = 2\pi n/T$, the above can be rewritten as,

$$F(t) = 1/2\ a_o + 1/2 \sum_{n=1}^{\infty} (a_n - ib_n)\ e^{i\omega_n t} + 1/2 \sum_{n=1}^{\infty} (a_n + ib_n)\ e^{-i\omega_n t} \quad (1.9)$$

$$a_n + ib_n = \frac{2}{T} \int_o^T F(t)\ e^{-i\omega_n t}\ dt, \quad n = 0,1,2,.... \quad (a)$$

$$a_n - ib_n = \frac{2}{T} \int_o^T F(t)\ e^{-i\omega_n t}\ dt, \quad n = 0,1,2,.... \quad (b) \quad (1.10)$$

Since the phase $\omega_n\ t$ is linear in n, the F(t) can be further written as

$$F(t) = 1/2 \sum_{n=\infty}^{-1} (a_{-n} - ib_{-n})\ e^{i\omega_n t} + 1/2\ a_o + \sum_{n=1}^{\infty} (a_n - ib_n)\ e^{i\omega_n t} \quad (1.11)$$

This permits the simpler, more compact, representation of any given function, F(t) as,

CE ...ARY
Acc. No. A. 118172

$$F(t) = 1/2 \sum_{-\infty}^{+\infty} (a_n - ib_n)\, e^{i\omega_n t} = \sum_{-\infty}^{\infty} C_n\, e^{i\omega_n t} \qquad (1.12)$$

where $C_n = 1/2\ (a_n - ib_n) = 1/T \int_o^T F(t)\, e^{-i\omega_n t}\, dt,$

$n = 0, \pm 1, \pm 2$ etc.

from the above it is clear that

$$a_{-n} = a_n. \qquad b_{-n} = -b_n \qquad n = 1,2,3, \ldots..$$

RELATIONSHIP TO THE CONTINUOUS TRANSFORMS

Much of the literature on wave propagation use Fourier integral on continuous transforms. It is of interest, therefore to show the relationship between it and Fourier series.

First, the series transform pair is rewritten

$$2\pi\, F(t) = \sum_{-\infty}^{\infty} (T\, C_n)\, e^{i\omega_n t}\, \Delta\omega, \quad T\, C_n = \int_t^T F(t)\, e^{-i\omega_n t}\, dt, \qquad (1.13)$$

where $\omega_n = 2\pi n/T$ and $\Delta\omega = 2\pi/T$. Now let the time window encompass from $-\infty$ to $+\infty$ consuming the signal is zero before time t = 0). Thus $\Delta\omega$ becomes $d\omega$ and the summation becomes an integral, that is

$$F(t) \rightarrow \sum_{-\infty}^{\infty} T\, C_n\, C\omega\ e^{i\omega_n t}\, d\omega, \quad T\, C_n\, (\omega) \rightarrow \int_{-\infty}^{+\infty} F(t)\, e^{-i\omega_n t}\, dt \qquad (1.14)$$

These are the Fourier continuous transforms. In the region of applicability, they have the correspondence

$T\, C_n \rightarrow C(\omega)$

An alternative scheme to set up the correspondence is to consider the C_o component for pulse and how it relates to C(o) of

the continuous transform.

DISCRETE FOURIER TRANSFORM

The discrete coefficients in the fourier series are obtained by performing continuous integrations over the time period. The integrations are now replaced by summations as a further step in the numerical implementation of the continuous transform.

APPROXIMATIONS FOR THE FOURIER COEFFICIENTS

The essential starting point for the discrete transform is the series transform pair rearranged as

$$F(t) = \frac{1}{T} \sum_{-\infty}^{\infty} C_n \, e^{i\omega_n t}, \quad C_n(\omega) = \int_o^T F(t) \, e^{-i\omega_n t} \, dt$$

Let the function F(t) be divided in M piecewise constant segments whose heights are f_m and base $\Delta T = T/M$. The coefficients are now obtained from

$$C_n \approx D_n = \sum_{m=0}^{M-1} f_m \int_{t_m - \Delta T/2}^{t_m + \Delta T/2} e^{i\omega_n t} \, dt = \Delta T \sum_m f_m \left\{ \frac{\text{Sin } \omega_n \Delta T/2}{\omega_n \Delta T/2} \right\} e^{i\omega_n t_m}$$

$$= \Delta T \left\{ \frac{\text{Sin } \omega_n \Delta T/2}{\omega_n \Delta T/2} \right\} \sum_m f_m \, e^{-i\omega_n t_m} \qquad (1.15)$$

It is seen that this is the sum of the transforms of a series of rectangles each shifted in times $t = t_m + \frac{\Delta T}{2}$. The contribution of each of these will now be evaluated more easily. If $n > m$,

i.e., $n = M + n^*$, where n is an exponential terms because

$$e^{-i\omega_n tn} = e^{-i\omega_{n_o} tm} = e^{-im\omega_o tm} \; e^{-in^*\omega_o tm} \qquad (1.16)$$

Hence the summation contribution simply becomes

$$\sum_{m=0}^{M-1} f_m \; e^{-in^*\omega_o tm}$$

Looking at the other contribution, it is seen that the Sinc function terms does depend on the value of n and is given by

$$\text{Sinc}(x) = \frac{\text{Sin}(x)}{x}, \quad x = \omega_n \Delta T/2$$
$$= \pi n \, f_o \Delta T$$
$$= \pi \, n \, \frac{1}{T} \frac{T}{M} = \pi \, \frac{n}{M}$$

Example 1 :

Let us consider a superimposed wave having the following representation :

$$y = a_1 \text{ Sin } (\omega_1 t + \phi_1) + a_2 \text{ Sin } (\omega_2 t + \phi_2) + a_3 \text{ Sin } (\omega_3 t + \phi_3) + b + z$$

where,

b	:	constant representing d-c component
a_1, a_2, a_3	:	amplitudes of waves ω_1, ω_2, ω_3 frequencies in order $\omega_1 < \omega_2 < \omega_3$.
ϕ_1, ϕ_2, ϕ_3	:	The phase differences.
z	:	a random sriable representing noise (assumed to be not more than 10% of the maximum signal).

We first consider a special form of eqn. (1a) where phase differences are taken as zero i.e., ϕ_1, ϕ_2, $\phi_3 = 0$. We have

generated the results for $a_1 = 1$, $a_2 = 2$, $a_3 = 3$ in figure A1a. The FFT of this curve has been carried out and given in figure A1b. In this fugure the position of the spikes give ω_t and the ordinate y_i gives a_1. For example if a_1 is taken as unity a_2 and a_3 are 2 and 3. This way it is that the signal is completely recovered.

Various filter are used to eliminate z and b and highlight the importance of ω_1, ω_2, ω_3. Now we can select any frequency and using proper filters we can eliminate rest of them i.e., using band pass filters we can go for ω_2, by low pass filter we can go for ω_1 and high pass filter for ω_3.

Now we will see effect of various windows in the regneration of signal : Here we have found that rectangular windows are not regenerating signals properly and with Hanning windows results are satisfactory. (Any window can't remove all the errors and noise so we will have to compromise in regeneration between amplitude and frequency. Since in our analysis frequencies have much important role to pay so we will select windows according to acceptable frequency regeneration).

In the examples presented in Fig. 1a shows the signal having noise, dc component and three frequencies which are 0.05, 1 and 7 Hz. So we will use low pass filter of order 11 for elimination of 7Hz frequency. Fig. A1a shows FFT magnitude response of crude signal which has three peaks corresponding to 0.05, 1 and 7 Hz frequencies. Fig. A1 c shows filtered FFT magnitude of signal with no peak for 7Hz frequency.

APPENDIX 2

SPECTRAL REPRESENTATION OF A TIME SIGNAL

Discrete time signal x(n) is periodic if for some positive value of N, where N is period of the signal,

$$x(n) = x(n+N) \tag{2.1}$$

The Complex exponential $e^{i(2\pi/N)n}$ is periodic with period N, i.e.,

$$\phi_k(n) = \phi_{k+N}(n)$$

where

$$\phi_k = e^{ik(2\pi/N)n} \tag{2.2}$$

we write x(n) as $x_n = \sum_{k=o}^{N-1} a_k e^{ik(2\pi/N)n}$ (2.3)

where the values of the function at different n values are

$$x_o = \sum_{k=o}^{N-1} a_k$$

$$x_1 = \sum_{k=o}^{N-1} a_k e^{2\pi ik/n}$$

.

.

.

$$x_{N-1} = \sum_{k=o}^{N-1} a_k e^{2\pi ik(N-1)/n}$$

If we wish to represent a Periodic Signal by a Fourier series, in the following we use eq. 2.3

$$\sum_{k=o}^{N-1} a_k \, e^{ik(2\pi/N)n} = 1 + e^{ik(2\pi/N)n} + e^{ik(2\pi/N)2} + \ldots e^{ik(2\pi/N)n} \tag{2.4}$$

$$= 1 + \alpha + \alpha^2 + \ldots + \alpha^{N-1}$$

$$\triangleq S$$

where

$$\alpha = e^{ik(2\pi/N)n}$$

Above S can take on discrete values as

$$S = \begin{cases} N & \text{when } \alpha = 1 \\ \left(\frac{1-\alpha^N}{1-\alpha}\right) & \text{when } \alpha \neq 1 \end{cases}$$

Now α will be equal to 1 when $e^{ik(2\pi/N)} = 1$ i.e. when k is a multiple of N (k = 0, ± N, ±2N, ...). In other words,

$$\sum_{n=o}^{N-1} a_k \, e^{ik(2\pi/N)n} = \begin{cases} N & \text{when } k = 0, \pm N, \pm 2N \\ 0 & \text{otherwise} \end{cases} \tag{2.6}$$

Now $x_n = \sum_{k=o}^{N-1} a_k \, e^{jk(2\pi/N)/n}$

$$\therefore \sum_{n=o}^{N-1} x_n \, e^{ir(2\pi/N)/n} = \sum_{n=o}^{N-1} \left[\sum_{k=o}^{N-1} a_k \, e^{ik(2\pi/N)(k-r)} \right] \tag{2.7}$$

$$= \sum_{k=o}^{N-1} a_k \left[\sum_{n=o}^{N-1} e^{i(2\pi/N)(k-r)n} \right]$$

$$= \sum_{k=o}^{N-1} a_k \begin{cases} N & \text{if } (k-r) = 0, \pm N, \ldots \\ 0 & \text{otherwise} \end{cases}$$

$$= \sum_{k=o}^{N-1} a_k \left(\delta_{kr\ N}\right) \left\{ \begin{array}{l} \text{since } k = 0, 1, \ldots N-1 \\ \qquad i = 0, 1, \ldots N-1 \end{array} \right.$$

where, $a_r = \frac{1}{N} \sum_{n=o}^{N-1} x_n\ e^{-ir(2\pi/N)n}$

The Fourier series coefficients a_k are often referred to as the spectral coefficients of x_n. These coefficients specify a decomposition of x_n into a sum of N harmonically related complex exponentials, we if take k in the range from 0 to (N-1), we have :

$$x_n = a_o\phi_o\ [n] + a_1\phi_1\ [1] + \ldots + a_{N-1}\ \phi_{N-1}\ [n] \qquad (2.9)$$

Similarly if we take k to range from 1 to N, we obtain

$$x_n = a_1\phi_1\ [n] + a_2\phi_2\ [n] + \ldots + a_N\ \phi_N\ [n] \qquad (2.10)$$

where,

$$\phi_k\ [n] = e^{ik(2\pi/N)n}$$

Thus,

$$\phi_{k+N}[n] = e^{i(2\pi/N)n(k+N)} = e^{i(2\pi Kn/N)}\ e^{i(2\pi nk)} = \phi_k[n] \qquad (2.11)$$

On comparing equation (2.9) and (2.10), we get (using the fact that $\phi_k\ [n] = \phi_{k+N}\ [n]$ hence $\phi_o\ [n] = \phi_k\ [n]$) :

$$a_o = a_N$$

Similarly by letting k range over any set of N consecutive integers and using $\phi_k = \phi_{k+N}$, we can conclude that

$$a_k = a_{k+N}$$

That is, if we consider more than N sequential values of k, the values of a_k will repeat periodically with period N. In particular, since there are only N distinct complex exponentials that are periodic will period N, the discrete time Fourier series representation is a finite series with N terms. Therefore if we fix the N consecutive values of k over which we define the Fourier series given below, we will obtain a set of exactly N Fourier coefficients from equation (2.13) as follows :

$$x_n = \sum_{k=o}^{N-1} a_k \, e^{ik(2\pi/N)/n} \qquad (2.12)$$

where,

$$a_n = \frac{1}{N} \sum_{n=o}^{N-1} x_n \, e^{-ik(2\pi/N)/n} \qquad (2.13)$$

Above equation (2.12) is synthesis equation whereas (2.13) is analysis equation. Furthermore since the ϕ_k [n] $\left[= e^{ik(2\pi/N)n} \right]$ repeat periodically with period N as we vary k, so must the a_k vary (since $a_k = a_{k+N}$).

Example 2.1 Consider the Signal

$$x_n = \text{Sin } r_o \, n \qquad (2.1.1)$$

There are three different situations, depending on whether $\frac{2\pi}{r_o}$ is an integer, a ratio of integers, or an irrational number, x_n is

periodic in the first two cases but not in the third. Consequently, the Fourier series representation of this signal applies only in the first two cases.

Case 1 : $\frac{2\pi}{r_o}$ is an integer N, $\rightarrow \frac{2\pi}{r_o} = N \rightarrow r_o = \frac{2\pi}{N}$

$$\rightarrow x[n] = \text{Sin } r_o n = \text{Sin } \frac{2\pi}{N} = \frac{1}{2i}\left[e^{i(2\pi/N)n} - e^{-i(2\pi/N)n} \right]$$

On comparing it with

$$x_n = \sum_{k=o}^{N-1} a_k \, e^{ik(2\pi/N)/n}$$

$$\rightarrow a_1 = \frac{1}{2i}, \quad a_{-1} = -\frac{1}{2i} \qquad (2.1.2)$$

The remaining coefficients over the interval of summation are zero. These coefficients repeat in the period N.

Example 2.2 : Let $x[n] = \text{Sin } (\frac{2\pi}{N})n$

Period of repetition N=5.

Case 2: $\frac{2\pi}{r_o}$ is a ratio of integers

$$\rightarrow \frac{2\pi}{r_o} = \frac{N}{m} \rightarrow r_o \left(\frac{2\pi m}{N}\right)$$

$$\rightarrow x_n = \text{Sin } r_o n = \text{Sin } \left(\frac{2\pi m}{N}\right) n$$

$$= \frac{1}{2i}\left[e^{i(2\pi m/N)n} - e^{-i(2\pi m/N)n} \right]$$

Compare with $x_n = \sum_{m=o}^{N-1} a_m \, e^{im(2\pi/N)/n}$

$$\rightarrow a_m = \frac{1}{2i}, \quad a_{-m} = -\frac{1}{2i}$$

Remaining coefficients over one period of length N are zero. The coefficients repeat with period N.

Example : Let $x[n] = \text{Sin}\ (\frac{2\pi}{5})n$

$$\rightarrow a_3 = \frac{1}{2i}, \quad a_{-3} = -\frac{1}{2i} \qquad (2.2.1)$$

Period of repetition = 5.

Example 2.3

Consider, the discrete time periodic square were

$$\text{From the figure } x_n = \begin{cases} 0 & -N/2 < n < -N_1 \\ 1 & -N_1 < n < N_1 \\ 0 & N_1 < n < N/2 \end{cases} \qquad (2.3.1)$$

$$\text{Use the relation } a_r = \frac{1}{N} \sum_{n=o}^{N-1} x_n\, e^{-ir(2\pi/N)/n}$$

$$a_r = \frac{1}{N} \sum_{n=o}^{N_1} 1.\ e^{-ir(2\pi/N)/n}$$

$$= \frac{1}{N} \left[e^{+ir(2\pi/N)/N_1} + e^{+ir(2\pi/N)/N_1}\ e^{-ir(2\pi/N)} + .. \right]$$

which is geometric series with $(2N_1 + 1)$ terms

$$a_r = \frac{1}{N}\ e^{ir(2\pi/N)N_1}$$

$$\text{or, } a_r = \frac{1}{N} \frac{e^{i(2\pi/N)N_1} \; e^{-ir(2\pi/N)(2N+1/2)} \; e^{-ir(2\pi/N)(2N+1/2)}}{e^{-ir(2\pi/N)1/2} \; [e^{ir(2\pi/2N)} - e^{ir(2\pi/2N)}}$$

$$\text{or, } a_r = \frac{1}{N} \frac{\text{Sin}\left[\frac{2\pi r}{N}\left[N_1 + \frac{1}{2}\right]\right]}{\text{Sin}\left[\frac{2\pi r}{2N}\right]}$$

if $e^{ir(2\pi/N)} \neq 0$ (2.3.2)

i.e. if $r \neq 0$

if $r = 0$ then the sum is

$$a_r = \frac{1}{N} \sum_{n=<N>}^{N_1} 1.1 = \left(\frac{2N_1+1}{N}\right) \quad \text{if } r = 0$$

Also $a_{r+N} = a_r$

This expression for the Fourier series coefficients can be written more completely if we express the coefficients as samples of an envelope

$$Na_k = \frac{\text{Sin}\,[(2N_1+1)r/2]}{\text{Sin}(r/2)} \Bigg|_{r = 2\pi k/N} \qquad (2.16)$$

Discrete Fourier Transform Pair

$$W_d\left(\frac{m}{NT}\right) = \sum_{n=o}^{N-1} \omega_d\,(nT)\, e^{-i(2\pi n/N)/m} \qquad (2.17)$$

$$\omega_d\,(nT) = \frac{1}{N} \sum_{m=o}^{N-1} W_d\left(\frac{m}{NT}\right) e^{-i(2\pi n/N)/m}$$

where,

T is sampling integral

Both ω_d and W_d are periodic with a periond N. In particular

$$W_d\left(\frac{m}{NT}\right) = W_d\left(\frac{m}{NT} + \frac{1}{T}K\right) \qquad (2.18)$$

$$\omega_d\,(nT) = \omega_d\,[\,(n \pm kN)\,T\,]$$

Example 2.4

$$\frac{2\pi}{r_o} = \frac{N}{ml} \rightarrow r_o\,\frac{2\pi}{N}\,m'$$

Also let

$$\omega_d\,(nT) = \text{Sin}\,\frac{2\pi}{N}\,nm' \quad (m' \text{ not necessairly an integer})$$

$$\omega_d\,(nT) = \frac{1}{2i}\left[\,e^{i(2\pi m'/n)N} - e^{-i(2\pi m'n/N}\right]$$

$$W_d\left(\frac{m}{NT}\right) = \sum_{n=o}^{N-1}\frac{1}{2i}\left\{\left[\,e^{-i(2\pi m'n/N)}\right]e^{-i(2\pi n/N)m} - e^{-i(2\pi nm'/N)}\,e^{-i(2\pi n/N)m}\right\}$$

$$W_d\left(\frac{m}{NT}\right) = \sum_{n=o}^{N-1}\frac{1}{2i}\left\{e^{-i(2\pi n/N)(m'+m)} - e^{-i(2\pi n/N)(m+m')}\right\}$$

$$= \frac{1}{2i}\left\{\frac{[1-e^{-i)2\pi/N)(m'+m)N}}{[1-e^{-i(2\pi/N)(m-m')}} - \frac{[1-e^{-i(2\pi/N)m'+m)N}}{[1-e^{-i(2\pi/N)(m-m')}}\right\}$$

Case 1 : Let $m \propto m'$ and $\frac{(m-m')}{N}\,2\pi$ be small

$$= e^{-i(2\pi n/N)(m+m')} = (1-p)\ (let) \text{ where } |p| \text{ is small}$$

$$p = \left[\,1 - e^{-i(2\pi n/N)(m+m')}\right] \quad p \text{ is complex in general}$$

$$W_d\left(\frac{m}{NT}\right) \propto \frac{1}{2i}\left\{\frac{1-(1-p)^r}{p}\right\}$$

$$= \frac{1}{2i}\left\{\frac{1 - (1-NP + \frac{N^2p^2}{2} \cdots}{p}\right\}$$

$$= \frac{1}{2i}\left\{\frac{NP - \frac{N^2p^2}{2} \cdots}{p}\right\} = \frac{1}{2i}\left\{N - \frac{N^2p}{2} \cdots\right\}$$

$$\frac{N}{2i}\left\{1 - \frac{p}{2}\right\}$$

$$\rightarrow \left\{1 - \frac{p}{2}\right\} = i\,\frac{W_d\,(m/NT)}{\{N/2\}}$$

$$\text{Now}(1-p) = 2\left\{1 - \frac{p}{2}\right\} - 1 = \left[2i\,\frac{W_d\,(m/NT)}{\{N/2\}} - 1\right]$$

$$= e^{-i(2\pi/N(m-m')}$$

$$e^{-i(2\pi/N(m-m')} = \text{Phase of } \left[2i\,\frac{W_d\,(m/NT)}{\{N/2\}} - 1\right] \text{ expressed in radious}$$

$$\Delta m = (m - m') = \frac{N}{2\pi}\left\{\text{Phase of } \left[2i\,\frac{W_d\,(m/NT)}{\{N/2\}} - 1\right]\right\} \text{ expressed in radious}$$

TABLE - A2

SOME EXAMPLES OF FILTERS

Low Pass Filters - They permit lower frequencies to pass through and the high frequencies are stopped, with a transition zone of passband and stopband (of frequencies).

We design such filters by choosing a finite, symmetric set of coefficients we select a digital filter of the form

$$y_n = \sum_{K=-N}^{kN} C_k \, U_{n-K} \qquad (C_k = C_{-k}) \qquad (2.1)$$

U_n = U(n) sampled value.

High Pass Filters - It passes the high frequencies and stops low. It can be called a difference between all pass filters and low pass filters.

We design it by simply replacing f in L.P. filters by (1/2-f) it changes sign of odd harmonics.

Bandpass and Bandstop Filters - They permit/restrict a particular range of frequencies. They have two transition zones.

NOTCH FILTERS - A very narrow band stop filter is called notch filter. Among other uses, a notch filter is used to remove the ever present 50 Hz that comes from electrical power distribution system.

Consequently the first zero occurs where n=M. This function is such that it decreases rapidly with n and is negligible beyond its first zero n=M. If M is made very large, that is, the

integration segments are very small, then it will be the higher order coefficients (i.e.,; large n) that are in the vicinity of the first zero. Let it be further assumed that the magnitude of these higher order coefficients is negligibly small. Then an approximation for the coefficients is

$$D_n \approx \Delta T \{1\} \sum_{m}^{M} f_m e^{-i\omega_n t_m} \qquad (2.2)$$

On the assumption that it is good for $n < m$ and $C_n \approx 0$ for $n \geq M$.

Since there is no point in evaluating the coefficient for $n > M-1$, then the approximation for the Fourier series coefficient (now called Discrete Fourier Transform) is taken as

$$f_m = f(t_m) \approx \frac{1}{T} \sum_{n=0}^{N-1} D_n e^{+i\omega_n t_m} = \frac{1}{T} \sum_{n=0}^{N-1} D_n e^{+i2\pi nm/N} \qquad (2.3)$$

$$D_n = D(\omega_n) \approx \Delta T \sum_{n=0}^{N-1} f_m e^{+i\omega_n t_m} = \Delta T \sum_{n=0}^{N-1} f_n e^{-i2\pi nm/N} \qquad (2.4)$$

where both m and n range from 0 to N-1. There are the definitions of the discrete Fourier Transform. Here the exponentials don't contain dimensional quantities, only the integers n,m,N. In this transform, both the time and frequency domains are discretized, and, as a consequence, the transform behaves periodically in both domains.

PROPERTIES OF DISCRETE TRANSFORM

$$t = t_m = m\Delta T \qquad (2.5)$$

$$\omega = \omega_n = 2\pi n/N\Delta T \qquad (2.6)$$

also $f_m = f(t_m)$ is the input signal for the discrete Fourier transform, while f(t) is the input signal for the continuous transform thus

$$C \Leftrightarrow D_n$$

That is, they both have the same magnitudes. This was achieved by choosing the appropriate scale factors of eqns. for approximate of the Fourier coefficient.

FAST FOURIER TRANSFORM

Final step in the numerical implementation is the development of an efficient algorithm for performing the summations of the discrete fourier transform. The fast fourier transform (FFT) is simply a very efficient scheme for computing the discrete Fourier transform. It is not the different transform.

ALIASING

The basic difference between the continuous and the discrete fourier transform is sampling (both rate and duration). An actual singla of very long duration must be truncated to a reasonable size before the discrete fourier transform is evaluated.

The transform of the signal will therefore be dependent on the actual function F(t) and the way it is sampled. Note that if the sampling rate is every ΔT, then the highest detectable frequency using the FFT is $1/(2\Delta T)$. Thus of ΔT is too large the highest detectable frequency using FFT is $1/2\Delta T$. Thus, if ΔT is too large the high frequency appears as a lower frequency cits alias) as shown in Fig. This phenomena of aliasing can be avoided if the sampling rate is high enough i.e., rate commensurate with

the highest significant frequency in the signal.

From the practical point of view, this is also avoided by recording with the analog filters set so as to remove significant frequencies above Nyquist.

LEAKAGE

The estimated spectrum is given only at discrete frequencies and this can cause another problem known as leakage. For example, suppose there is a special peak at 117 KHz and the sampling is such that the spectrum values are only at every 15 KHz. Then the energy associated with the 117 KHz peak leaks into the neighbouring frequencies, thus distoring their spectral estimates.

Leakage is most significant in instances where the signal has sharp spectral peaks and is least significant in cases where signal is a flat, bread - banded signal. In the analysis of the impact of structures, the signals generated generally don't exhibit spectral peaks (as in case of vibrations). However, it can become a problem if there are many reflections present in the signal.

PADDING

Since discrete fourier analysis represets a finite sample of an infinite signal on a finite period. Then schemes for increasing the apparent period must be used. The simplest means of doing this is by padding.

There are various ways of padding the signal and the one most commonly used is that of simply adding zeroes.

The main consequence of padding is that since a large time window is used them higher resolution in the frequency domain in

achieved. It also makes the signal non-periodic over a large time domain. There effects can be seen.

As regards padding with zeroes it should be pointed out that it really doesn's matter if the zeroes are before the recorded signal or after thus even if the signal never decrease to zero, padding is justified because it represents the only quiescent part of the signal.

APPENDIX 3


```
5   REM
6   REM _________Program to transfer time data from AD-3525 FFT Analyser_____
7   REM ==========================================================================
8   REM
10  CLS : LOCATE 4, 7, 1, 0, 31
15  REM PLAY "o2l16e-9n0e-d-d-n0e-n0e-d-d-d-n0e-9n0e-d-d-n0e-"
20  PRINT " P R O G R A M    T O    T R A N S F E R    T I M E    D A T A "
30  PRINT
40  REM ...decl.bas...
50  CLEAR , 60000!
60  IBIN         IT1 = 60000!: IBINIT2 = IBINIT1 + 3: BLOAD "bib.m", IBINIT1
70  CALL IBINIT1(IBFIND, IBTRG, IBCLR, IBPCT, IBSIC, IBLOC, IBPPC, IBBNA,
                 IBONL, IBRSC, IBSRE, IBRSV, IBPAD, IBSAD, IBIST, IBDMA,
                 IBEOS, IBTMO, IBEOT, IBRDF, IBWRTF, IBTRAP)
80  CALL IBINIT2(IBGTS, IBCAC, IBWAIT, IBPOKE, IBWRT, IBWRTA, IBCMD, IBCMDA,
          IBRD, IBRDA, IBSTOP, IBRPP, IBRSP, IBDIAG, IBXTRC, IBRDI,
          IBWRTI, IBRDIA,  IBWRTIA, IBSTA%, IBERR%, IBCNT%)
90  REM ....assigning a unique identifier to device and storing it in DVM%
100 BDNAME$ = "KIK"
110 CALL IBFIND(BDNAME$, DVM%)
120 REM
130 REM          ....checking for error on IBFIND call.
140 IF DVM% < 0 THEN GOSUB 820
150 REM
160 REM          ....clearing device.
170 CALL IBCLR(DVM%)
180 IF IBSTA% < 0 THEN GOSUB 830
200 REM
210 REM ....setting sensitivity range to +10dBV.
220 WRT$ = "FRQ13 SNA8 SNB8 TDM1 TLN6 TGS0 ": CALL IBWRT(DVM%, WRT$)
225 IF IBSTA% < 0 THEN GOSUB 840
230 WRT$ = "VDS1 VUL1 VAB1 VUL0 VAB0 TPV0.000 TRP0 TRG1 " : CALL IBWRT(DVM%,WRT$)
240 IF IBSTA% < 0 THEN GOSUB 850
250 PRINT "IBSTA% after initialising = "; IBSTA%
260 CNT% = 4096
270 CNT% = CNT% /2
280 DIM IAR%(5000): FLAG = 0
290 PLAY "MB0O0L32A-L64CL16BL64A+"
340 INPUT "Press a key after collecting data ";JUNK$
341 REM
343 PLAY "MBo0L32A-L64CL16BL64A+"
344 PRINT:INPUT "File name for Channel A data --> ",FLA$
345 PRINT:INPUT "File name for Channel B data --> ",FLB$
350 CLS: FOR J = 0 TO CNT2%: IAR%(J) = 0: NEXT J
355 WRT$ = "THL1 TAR 00-1023? "  : CALL IBWRT(DVM%,WRT$)
360 IF IBSTA% < 0 THEN GOSUB 860
375 F$=FLA$
380 GOSUB 900
385 REM
395 PLAY "MBo0L32A-L64CL16BL64A+"
415 CLS: FOR J = 0 TO CNT2%: IAR%(J) = 0: NEXT J
420 WRT$ = "THL1 TBR 00-1023? "  : CALL IBWRT(DVM%,WRT$)
425 IF IBSTA% < 0 THEN GOSUB 870
427 F$=FLB$
430 GOSUB 900
434 REM
435 REM --------------Releasing FFT Analyser----------------
440      CALL IBCLR(DVM%)
445      IF IBSTS% < 0 THEN GOSUB 875
450      V% = 1: CALL IBONL(DVM%, V%)
455      IF IBSTA% < 0 THEN GOSUB 880
460 PRINT: PRINT
462 PLAY "MBo0L32A-L64CL16BL64A+"
465 LOCATE 16, 21, 1, 0, 31: INPUT " DO YOU WISH TO CONTINUE (Y/N) ? ", YES$
470 IF YES$ = "Y" THEN GOTO 10
475 END
```

```
492 REM
495 REM
500 REM ////////////////////Error Messages//////////////////////
505 REM
820     PRINT "IBFIND call error": RETURN
830     PRINT "IBCLR call error": RETURN
840     PRINT "1st IBWRT call error": RETURN
850     PRINT "2nd IBWRT call error": RETURN
860     PRINT "Channel A's IBWRT call error": RETURN
870     PRINT "Channel B's IBWRT call error": RETURN
875     P         RINT "IBCLR call error while releasing FFT": RETURN
876     PRINT "IBRDI call error": RETURN
880 REM
885 REM
900 REM ///////////////Subroutine for processing & writing data////////////////
910 REM
915 REM
920 CALL IBRDI(DVM%, IAR%(0), CNT%)
923 IF IBSTA% < 0 THEN GOSUB 876
925 PRINT "NO. OF BYTES AFTER IBRDI = ";IBCNT%
930 PLAY "MBo0L32A-L64CL16BL64A+"
940 CLS : LOCATE 12,20,0,0,31: PRINT " TRANSFERRING  DATA.  PLEASE  WAIT ..."
990 OPEN F$ FOR OUTPUT AS #1
1010 FOR J = 0 TO (CNT2% -2) STEP 2
1020 BYTE1% = IAR%(J) AND 255
1030 BYTE2% = (IAR%(J) AND 32512) \ 256
1040 REM
1050 REM ...the leftmost byte, BYTE2%, is the sign-byte...
1060 IF IAR%(J) < 0 THEN BYTE2% = BYTE2% + 128
1080 BYTE3% = IAR%(J + 1) AND 255
1090 BYTE4% = (IAR%(J + 1) AND 32512) \ 256
1100 REM
1110 REM ...the leftmost byte, BYTE4%, is the sign-byte...
1120 IF IAR%(J + 1) < 0 THEN BYTE4% = BYTE4% + 128
1150 S% = (BYTE1% AND 128) \ 128
1160 N1% = BYTE1% AND 127
1170 L7% = (BYTE2% AND 128) \ 128
1180 EE1 = N1% * 2
1190 EE2 = L7%
1200 EE = EE1 + EE2
1220 N2% = BYTE2% AND 127
1230 F1 = N2% / 128
1240 F2 = BYTE3% / 32768!
1250 F3 = BYTE4% / 8388608!
1260 F = F1 + F2 + F3
1270 IF (S% = 0 AND EE = 0 AND F = 0!) THEN 1280 ELSE 1300
1280 VOLT = 0
1290 GOTO 1350
1300 EX = EE
1310 TT = 2 ^ (EX - 127)
1330 VOLT = (1! + F) * TT
1340 IF S% <> 0 THEN VOLT = -VOLT
1350 REM
1400 PRINT #1, VOLT
1410 SOUND 200, .025
1420 NEXT J
1430 CLOSE #1
1440 PLAY "MBT160O1L8CDEDCDL4ECC"
1450 CLS : LOCATE 11, 22, 1, 0, 31: PRINT " DATA TRANSFERRED TO", F$
1460 RETURN
```